Title: Antiviral *Wolbachia* strains associate with *Aedes aegypti* endoplasmic reticulum membranes and disturb host cell lipid distribution to restrict dengue virus replication

Robson K. Loterio[1], Ebony A. Monson[2*], Rachel Templin[3*], Jyotika T. Bruyne[4], Heather A. Flores[5] Jason M. Mackenzie[6], Georg Ramm[3], Karla J. Helbig[2], Cameron P. Simmons[1,4], Johanna E. Fraser[1#]

[1]Department of Microbiology, Biomedicine Discovery Institute, Monash University, Clayton, Australia; [2]Department of Physiology, Anatomy, and Microbiology, School of Life Sciences, La Trobe University, Melbourne, Australia; [3]Ramaciotti Centre For Cryo-Electron Microscopy, Monash University, Clayton, Australia; [4]World Mosquito Program, Monash University, Clayton, Australia; [5]School of Biological Sciences, Monash University, Clayton, Australia; [6]Department of Microbiology and Immunology, University of Melbourne at the Peter Doherty Institute for Infection and Immunity, Melbourne, Australia. *These authors contributed equally.

Corresponding author: johanna.fraser@monash.edu

Abstract: The insect endosymbiotic bacterium *Wolbachia pipientis* is being utilised as a biocontrol tool to reduce the incidence of *Aedes aegypti*-transmitted viral diseases like dengue. However, the precise mechanisms underpinning *Wolbachia*'s antiviral activity are not well defined. Here we generated a panel of *Ae. aegypti*-derived cell lines infected with antiviral strains *w*Mel and *w*AlbB or the non-antiviral strain *w*Pip to understand host cell morphological changes specifically induced by antiviral strains. Antiviral strains were frequently found to be entirely wrapped by the host endoplasmic reticulum (ER) membrane, while *w*Pip bacteria clustered separately in the host cell cytoplasm. ER-derived lipid droplets (LDs) increased in volume in *w*Mel- and *w*AlbB-infected cell lines and mosquito tissues compared to cells infected with *w*Pip or *Wolbachia*-free controls. Inhibition of fatty acid synthase (required for triacylglycerol biosynthesis) reduced LD formation and significantly restored ER-associated dengue virus replication in cells occupied by *w*Mel. Together, this suggests that antiviral *Wolbachia* strains may specifically alter the lipid composition of the ER to preclude the establishment of DENV replication complexes. Defining *Wolbachia*'s antiviral mechanisms will support the application and longevity of this effective biocontrol tool that is already being used at scale.

Importance: *Aedes aegypti* transmits a range of important human pathogenic viruses like dengue. However, infection of *Ae. aegypti* with the insect endosymbiotic bacterium, *Wolbachia*, reduces the risk of mosquito to human viral transmission. *Wolbachia* is being utilized at field sites across more than 13 countries to reduce the incidence of viruses like dengue, but it is not well understood how *Wolbachia* induces its antiviral effects. To examine this at the subcellular level, we compared how different strains of *Wolbachia* with varying antiviral strengths, associate with and modify host cell structures. Strongly antiviral strains were found to specifically

associate with the host endoplasmic reticulum and induce striking impacts on host cell lipid distribution. Inhibiting *Wolbachia*-induced lipid redistribution partially restored dengue virus replication demonstrating this is a contributing role for *Wolbachia*'s antiviral activity. These findings provide new insights into how antiviral *Wolbachia* strains associate with and modify *Ae. aegypti* host cells.

1. Introduction

Arthropod-borne viruses (arboviruses) including dengue (DENV), Zika (ZIKV), chikungunya (CHIKV), and yellow fever virus (YFV), are primarily transmitted by female *Aedes aegypti* and, to a lesser extent, by female *Aedes albopictus* [1-3]. The global spread of these viruses has dramatically increased in recent decades. This is largely due to factors associated with the geographic distribution of *Aedes* spp. such as climate change [4-7], globalization [8,9], urbanization [9,10], resistance to insecticides [11], and the lack of effective vector control strategies [12].

A promising biological vector control strategy that has emerged in the last decade employs *Wolbachia pipientis* to restrict mosquito-to-human transmission of *Ae. aegypti*-borne viruses [13-17]. *Wolbachia* is an intracellular gram-negative endosymbiotic bacterium that infects a wide range of invertebrates, including arthropods and nematodes, but it is not naturally found in *Ae. aegypti* mosquitoes [18,19]. *Wolbachia* strains can be isolated from native hosts such as *Drosophila melanogaster* (*w*Mel) [14,20] and *Ae. albopictus* (*w*AlbB) [15,21,22], and then introduced into heterologous arthropods including *Ae. aegypti*. Strains such as *w*Mel and *w*AlbB induce an antiviral state in *Ae. aegypti* reducing the rate of infection, dissemination, and transmission of +RNA viruses such as DENV [14,20,23]. *Wolbachia*'s exceptional ability to infect and alter the host germ line to facilitate their vertical transmission through the maternal lineage underpins the application of this bacterium as a biocontrol tool[14]. Additionally, many *Wolbachia* strains are capable of inducing

77 cytoplasmic incompatibility (CI), a condition that gives *Wolbachia*-carrying females a
78 reproductive advantage [24,25]. These strains can be introgressed into wild-type *Ae.*
79 *aegypti* populations to reduce their transmission potential. This approach has been
80 shown to dramatically and significantly reduce the incidence of dengue in
81 communities [26-31].

82 DENV is a member of the *Flaviviridae* family with a single positive-strand RNA
83 genome that is surrounded by the virally encoded capsid protein in a host-derived
84 lipid bilayer [3,32]. The viral genome is released into the host cell cytosol after entering
85 susceptible cells via endocytosis and is translated by host machinery at the rough
86 endoplasmic reticulum [33,34]. DENV induces drastic rearrangements of endoplasmic
87 reticulum (ER) membranes to form viral replication complexes that are critically
88 required to coordinate the multiple steps of viral replication, genome translation, and
89 virion assembly [33-39]. *Wolbachia*'s antiviral impacts are believed to be systemic in
90 mosquitoes[40], but also cell autonomous whereby *Wolbachia*-infected cells do not
91 protect surrounding *Wolbachia*-free cells from viral infection [41]. At the subcellular
92 level, viral restriction is believed to occur early, before viral replication is effectively
93 initiated [42], and low levels of progeny virus produced in the presence of *Wolbachia*
94 have reduced infectivity [43]. How *Wolbachia* induces these antiviral effects is not well
95 understood, but a variety of hypotheses have been examined. These include
96 competition between *Wolbachia* and viruses for nutrients and physical space within
97 host cells [13,44-48], and altered expression of host pro- or antiviral genes [49-52], including
98 priming of immune pathways [23,53,54]. Implicating the mechanisms that drive the
99 *Wolbachia*-induced antiviral state has been difficult due to technical limitations such
100 as failure to genetically modify *Wolbachia* and to grow it axenically. However, new
101 experimental models may help to advance our understanding of *Wolbachia*-induced

host phenotypes. Specifically, we recently found that *Wolbachia* strain *w*Pip (derived from *Culex quinquefasciatus*) does not inhibit flavivirus replication, dissemination or transmission in *Ae. aegypti* [23,55]. We hypothesized that pairwise comparisons between *Ae. aegypti* infected with *Wolbachia* strains that do or do not induce an antiviral state may facilitate the dissociation of *Wolbachia*'s antiviral effects from the general symbiont effects. Here we generated a unique panel of *Ae. aegypti*-derived cell lines infected with *w*Mel, *w*AlbB (the antiviral stains being utilized in *Ae. aegypti* biocontrol programs) or *w*Pip to identify the subcellular changes specifically induced by antiviral *Wolbachia* strains. We identify intimate *Wolbachia*-ER interactions and triacylglyceride biosynthesis for LD formation as key host cell modifications that contribute to the *Wolbachia*-induced antiviral state.

2. Results

2.1 – Generation of a panel of *Wolbachia*-infected *Ae. aegypti*-derived cell lines

To examine the subcellular changes specifically induced by antiviral *Wolbachia* strains, we generated a panel of *Wolbachia*-infected cell lines using the immunocompetent *Ae. aegypti*-derived cell line (*Aag2*). *Aag2* cells infected with antiviral strain *w*Mel and the *w*Mel-cured line (*w*Mel.Tet-*Aag2*) have been described previously [56]. *w*AlbB-*Aag2* and *w*Pip-*Aag2* cell lines were produced by stable infection of *w*Mel.Tet-*Aag2* using *Wolbachia* isolated from previously generated cell lines (RML12-*w*AlbB) or *Ae. aegypti* eggs (Rockefeller-*w*Pip). This was done to account for insect-specific flaviviruses known to infect *Aag2* cells but not *w*Mel-*Aag2* or *w*Mel.Tet-*Aag2* (herein referred to as *Wolbachia*-free-*Aag2*) [57].

126 To confirm that *w*AlbB and *w*Pip had antiviral and non-antiviral impacts in
127 these cell lines, respectively, we evaluated DENV-2 replication in *Wolbachia*-free,
128 *w*Mel-*Aag2*, *w*AlbB-*Aag2* and *w*Pip-*Aag2* cells. Consistent with our previous findings
129 in *Ae. aegypti* [23,55], *w*Pip did not restrict DENV-2 replication or production of
130 infectious virus compared to the *Wolbachia*-free line (Fig. 1A & B). Notably, *w*Pip
131 was found to grow to a higher density than *w*Mel and *w*AlbB (average of 96
132 *Wolbachia* per cell, compared to 30 and 69 for *w*Mel and *w*AlbB, respectively) (Fig.
133 1A, in parentheses). By contrast, DENV-2 RNA copies and infectious virus were
134 significantly reduced by *w*Mel's potent antiviral activity (approximately 3 $\log_{10}$
135 reduction compared to *Wolbachia*-free). *w*AlbB also significantly inhibited DENV-2
136 replication and infectious virus in *Aag2* cell lines but the antiviral activity was weaker
137 than *w*Mel (approximately 1 $\log_{10}$ reduction compared to *Wolbachia*-free). This
138 confirms that the diverse antiviral phenotypes of *Wolbachia* strains previously
139 demonstrated in *Ae. aegypti* mosquitoes [20,22,23], can be recapitulated in *Aag2* cell
140 lines.

141 **2.2 – Antiviral *Wolbachia* strains associate with host ER membranes**

142 *Wolbachia* and viruses are both obligate intracellular residents of eukaryotic
143 cells that rely on a variety of host structures and processes to complete their life
144 cycles. Interestingly, *Wolbachia* titers and intracellular distribution have been shown
145 to be influenced by the host's genetic background [46,58,59]. To gain insights into how
146 *Wolbachia* strains may associate with *Ae. aegypti* cells to induce an antiviral
147 phenotype, we assessed our panel of *Aag2* cell lines using transmission electron
148 microscopy (TEM). Micrographs of the three *Wolbachia*-infected mosquito cell lines
149 show each cell line is heavily infected with their respective *Wolbachia* strain (top row,
150 Fig. 2A and Supplementary Fig. 1). *Wolbachia* appeared similar in size and shape to

151 mitochondria but could be differentiated by a lower electron density and an absence
152 of cristae. We observed that antiviral strains, *w*Mel and *w*AlbB, were frequently
153 associated with host membranes that appeared to be the host endoplasmic reticulum
154 (ER), while the non-antiviral strain *w*Pip was not (bottom row, Fig. 2A and
155 Supplementary Fig. 1e-p). By scoring the closeness of interaction between
156 *Wolbachia* and the ER a striking difference was evident between antiviral and non-
157 antiviral strains: approximately 50% of *w*Mel and *w*AlbB bacteria were in close
158 contact with ER membranes in *Aag2* cell lines. Of those, 25% were clearly
159 surrounded by the membranes (Fig. 2B & C). This tight association was observed in
160 our reconstructed tomograms of *w*Mel where the bacterium was found to be
161 surrounded by the ER double membrane, and in some instances was wrapped
162 multiple times (Fig. C – See Supplementary Movie 1 for the reconstructed
163 tomogram). Meanwhile, over 75% of *w*Pip bacteria were not located near any
164 intracellular membranes, and only 25% were situated adjacent to any part of the ER
165 (Fig. 2B and Supplementary Fig. 1m-p). To further confirm that the membrane
166 structures were indeed ER, we carried out live cell imaging using an ER tracker dye
167 which binds to the sulfonylurea receptors of ATP-sensitive K^+ channels present on
168 ER membranes, and SYTO11 which preferentially stains *Wolbachia* DNA over
169 eukaryote DNA [58,60]. Confocal fluorescence imaging confirmed the antiviral strains
170 *w*Mel and *w*AlbB exhibited substantial colocalization with ER membranes (white
171 arrowheads, Fig. 2D), while *w*Pip did not, instead forming a massive cluster of
172 cytosolic *Wolbachia* (Fig. 2D).

173 DENV and other flaviviruses significantly remodel ER membranes to form
174 replication complexes [32,33,35,36,61]. To determine whether the distinct ER interaction of
175 antiviral *Wolbachia* strains precludes DENV-2 association with the host ER we

176 infected each *Aag2* cell line with DENV-2 and performed TEM analyses. We
177 observed numerous viral replication sites containing many viral vesicle packets (Vp)
178 in the cytosol of the *Wolbachia*-free line (white arrowheads, Fig. 2E), consistent with
179 the high viral titers determined in this cell line (Fig. 1). We found no evidence of virus
180 replication in any of the *w*Mel-*Aag2* cell line micrographs examined, and few and
181 smaller Vp were observed in the *w*AlbB-*Aag2* cell line (white arrowheads, Fig. 2E).
182 Further consistent with our data in Fig. 1, *w*Pip showed numerous Vp in the cytosol,
183 similar to the *Wolbachia*-free control (white arrowheads, Fig. 2E). Together this
184 dataset provides the first insight into how antiviral *Wolbachia* strains differentially
185 associate with *Ae. aegypti* ER membranes and prevent formation of typical DENV-2
186 replication complexes.

187 **2.3 – Antiviral *Wolbachia* strains increase lipid droplet formation in *Aag2***
188 **cells**

189 It has previously been reported that the ER-derived organelle, lipid droplets
190 (LDs) are upregulated following DENV infection, contributing to the cellular antiviral
191 response in both mammalian and *Ae. aegypti*-derived cell lines [62,63]. Since the ER
192 provides most of the constituent molecules for LDs [64], we next hypothesised that the
193 association of antiviral *Wolbachia* strains with host ER membranes could further
194 manipulate other intracellular lipid sources.

195 To examine intracellular LDs, we stained all *Aag2* cell lines with BODIPY
196 493/503 and analyzed the number and size of LDs per cell. Notably, compared to the
197 *Wolbachia*-free line, all *Wolbachia*-infected lines induced LD accumulation (Fig. 3A &
198 B). Interestingly, *w*Mel induced the accumulation of a similar number of LD's per cell
199 as *w*Pip (27 and 30.2 per cell, respectively), while *w*AlbB induced near twice the
200 amount (50.5 per cell). However, *w*Mel-induced LDs were significantly larger than

201 those induced by *w*AlbB and *w*Pip (791.5, 417.5, and 365.5 nm respectively) (Fig.
202 3B). This implies that antiviral *Wolbachia* strains might boost the total volume of LDs
203 per cell.

204 Lipid biosynthesis and degradation play a role in several stages of DENV
205 infection, including viral replication, assembly, and energy supply [35,65-67]. Similarly,
206 *Wolbachia* proliferation is tightly associated with changes in the host lipidome [68-70].
207 Next, we investigated whether DENV-2 infection affected LD accumulation in the
208 presence of each *Wolbachia* strain. In line with previous findings [62], DENV-2 induced
209 the accumulation of LDs in *Wolbachia*-free cells (Fig. 3C & D). Interestingly, DENV-2
210 infection caused a further accumulation of LDs in *w*Mel-*Aag2* and *w*AlbB-*Aag2*, but
211 not in *w*Pip-*Aag2* (Fig. 3D). Furthermore, the LD accumulation observed in both cell
212 lines with antiviral *Wolbachia* strains after DENV-2 infection was significantly higher
213 than the LD accumulation in *Wolbachia*-free cells infected with DENV-2 (Fig. 3D). By
214 contrast, we measured similar levels of LDs in *w*Pip- and *Wolbachia*-free *Aag2* cells
215 infected with DENV-2 (22.5 and 21.7 per cell, respectively) (Fig. 3D), indicating an
216 association between high LD numbers and restriction of DENV-2 replication.

217 To investigate LD accumulation induced by different *Wolbachia* strains *in vivo*,
218 we dissected female *Ae. aegypti* infected with *w*Mel, *w*AlbB or *w*Pip. We selected
219 ovarian tissue since this tissue is rich in *Wolbachia* for all strains of interest
220 (Supplementary Fig. 2) [23]. Ovaries were stained with BODIPY 493/503 for LDs and
221 DAPI to demarcate nuclei. Supporting our *in vitro* findings, LDs were most prevalent
222 in the presence of antiviral *Wolbachia* strains compared to the *Wolbachia*-free
223 control (Fig. 3E). Taken together, our findings demonstrate that changes in
224 intracellular lipid storage are key features of mosquito cells infected with antiviral
225 *Wolbachia* strains.

226 **2.4 - Intracellular redistribution of lipids contributes to DENV-2 restriction in**
227 ***w*Mel-*Aag2* cells**

228 We next hypothesized that *Wolbachia*-induced LD formation may be required
229 to induce an antiviral state. A variety of small molecule inhibitors targeting
230 mammalian enzymes involved in LD formation were applied to *w*Mel- and
231 *Wolbachia*-free-*Aag2* cells to identify inhibitors that were effective against *Ae.*
232 *aegypti* orthologs. The DGAT 1 inhibitor (T863) and DGAT 2 inhibitor (PF-06424439)
233 did not reduce LD formation in these cells, but the fatty acid synthase (FAS) inhibitor
234 C75 did (Supplementary Fig. 3A & B). FAS is an enzyme that catalyzes the second
235 step of the *de novo* triacylglycerol synthesis pathway contributing to lipid storage (LD
236 formation) and membrane synthesis [71,72].

237 We therefore compared DENV-2 replication and infectious virus production in
238 *Wolbachia*-free and *w*Mel-*Aag2* cell lines treated with C75. While C75 treatment
239 reduced LD numbers in both cell lines DENV-2 replication was significantly reduced
240 only in *Wolbachia*-free cells (by ~1 $\log_{10}$), consistent with previous reports of LDs
241 playing a key role in DENV replication [67] (Fig. 4A, B & C). By contrast, C75
242 treatment of the *w*Mel-*Aag2* cell line partially restored DENV-2 replication, with
243 intracellular DENV-2 and infectious virus ~1 $\log_{10}$ higher than in untreated *w*Mel-
244 *Aag2* cells. Notably, C75 treatment of *w*Mel-*Aag2* cell lines did not reduce *Wolbachia*
245 density (Fig. 4A & B, in parentheses), indicating that FAS and *w*Mel-induced LDs are
246 not directly required for active *Wolbachia* replication and maintenance. However, it is
247 possible that prolonged periods of LD depletion could affect *Wolbachia* survival.

248 Finally, TEM micrographs of both *Wolbachia*-free and *w*Mel-*Aag2* cell lines
249 treated with C75 were examined to verify whether DENV-2 replication could now be

250 supported in cells near *w*Mel bacterium. We observed a reduction in visible cytosolic
251 Vps in the *Wolbachia*-free cell line, while, for the first time, we were able to find
252 evidence of virus replication in cells already occupied by *w*Mel (Fig. 4E). Together,
253 these data show that blocking the *de novo* lipogenesis of triacylglycerol significantly
254 compromises *w*Mel-induced LD accumulation, and consequently, its antiviral activity
255 in *Ae. aegypti* cells.

256 **Discussion**

257 *Wolbachia* has been implemented as a biocontrol tool in cities in Oceania,
258 Asia, and Latin America. Several epidemiological studies have now demonstrated
259 the efficacy of *Wolbachia*-introgression in reducing the burden of mosquito-borne
260 diseases in communities [26-31] and the Vector Control Advisory Group to the World
261 Health Organization has endorsed its public health value [73]. To best support the
262 longevity of this method, and to predict the emergence of *Wolbachia*-resistant
263 viruses, it is critical that we understand the mechanisms that underpin the antiviral
264 activity of *Wolbachia*.

265 Given that *Wolbachia* strains are classified into major phylogenetic lineages
266 known as supergroups [74], we can strategically compare host modifications induced
267 by the antiviral strain *w*AlbB and the non-antiviral strain *w*Pip because they both
268 belong to supergroup B. Additionally, both strains are adapted to mosquito host
269 species [74,75]. *w*Mel, which belongs to supergroup A [74], has a well-characterized
270 antiviral activity and comparisons with *w*AlbB enable us to determine whether
271 antiviral strains from different supergroups employ similar strategies to induce the
272 antiviral state in *Ae. aegypti*. In our cell culture models, we observed that supergroup
273 B strains, *w*AlbB and *w*Pip, grew to substantially higher densities (>80
274 *Wolbachia*/cell) than the distantly related *w*Mel (<30 *Wolbachia*/cell). This is

275 consistent with somatic tissues in mosquitoes where it has been reported that *w*AlbB
276 and *w*Pip generally reside at higher levels than *w*Mel [20,23,55]. Thus, our *in vitro*
277 findings support previous research and show that *Wolbachia* density does not
278 necessarily determine a strain's antiviral activity.

279 Recent investigations have demonstrated that *w*Mel resides nearby ER and
280 Golgi organelles in its native host, *D. melanogaster* [46,47,58]. Here, we remarkably
281 observed that only antiviral *Wolbachia* strains associate closely with the ER network
282 in *Aag2* cell lines. Non-antiviral strain *w*Pip instead formed a massive cytoplasmatic
283 cluster with no apparent interaction with other organelles. TEM analyses revealed
284 *w*Mel and *w*AlbB were individually surrounded by ER membranes at a high
285 frequency. This may be strategic by these strains; for example, the *w*Mel genome
286 lacks pathways for metabolizing some membrane components, relying on its host for
287 many of the materials required for their membrane formation [76-78]. Since *w*Pip does
288 not demand this close association for its active replication, perhaps it has alternate
289 ways of acquiring nutrients or has a more complete intrinsic metabolic capacity.
290 Comparative genomic studies between related strains *w*AlbB and wPip may provide
291 insight into this. Interestingly, based on our TEM micrographs, even in *Aag2* cell
292 lines highly infected with *w*AlbB or *w*Pip strains (>80 *Wolbachia*/cell), we did not see
293 any morphological evidence of increased ER activity linked to ER stress, such as
294 enlarged tubules and cisternae, nor subcellular redistribution of this organelle as
295 previously described for *w*Mel in *D. melanogaster* [46,47].

296 DENV and other flaviviruses considerably remodel ER membranes for their
297 own replication [32,33,35,36,61]. While it is interesting that only the antiviral *Wolbachia*
298 strains were found to be substantially associated with this organelle, our TEM
299 analyses did not indicate any spatial competition between antiviral *Wolbachia* strains

300 and DENV-2 for ER membranes. Indeed, ER membranes are prolific in eukaryotic
301 cells and we observed large regions of *Aag2* cells that had ER membranes free from
302 *Wolbachia*, with space to hypothetically support formation of viral replication
303 complexes. Instead, we hypothesize that antiviral *Wolbachia* strains may
304 biochemically alter the composition of the ER membranes in *Aag2* cells by eliciting
305 the formation of LDs. LDs may then have further direct or indirect roles in mediating
306 viral restriction.

307 LDs are thought to have conflicting roles in viral infection: many reports have
308 demonstrated that enveloped viruses usurp LDs and alter lipidomic profiles of host
309 cells to enhance their viral life cycles, with lipids accounting for 20-30% of the weight
310 of the virion [62,67,79-83]. DENV infection, for example, increases LD formation [62],
311 recruiting FAS to the virus replication site [65], and its capsid protein accumulates on
312 the surface of LDs, facilitating viral replication by providing a platform for
313 nucleocapsid formation during encapsidation [67]. By contrast, LDs have been shown
314 to have a critical role in supporting innate immune signaling pathways, potentially
315 acting as a platform to augment and coordinate the cell's antiviral response [62,63,84,85].
316 Since recent studies have suggested that *Wolbachia*'s antiviral activity towards
317 DENV is not driven by innate immune priming [23,53] it remains unclear what role
318 *Wolbachia*-induced LDs may have in viral restriction.

319 In this study we noticed distinct LD profiles in *Aag2* single-infected with
320 *Wolbachia* strains. Antiviral *Wolbachia* strains induced a higher volume of LDs per
321 cell than *w*Pip. Additionally, we found that *w*Mel- and *w*AlbB-*Aag2* cell lines
322 responded to DENV-2 infection by further accumulating LDs, which did not occur in
323 *w*Pip-*Aag2* cell line. Based on these findings, it appears that DENV-2 replication in
324 *Aag2* cell lines requires a preferred LD accumulation threshold that, if crossed, e.g.

325 in the presence of antiviral *Wolbachia* strains, no longer supports DENV-2
326 replication. Previously, *Aag2* cells infected with *w*MelPop (a supergroup A
327 pathogenic antiviral *Wolbachia* strain from *D. melanogaster*) were shown to have
328 LDs enriched in esterified cholesterol. DENV-2 replication was partially rescued in
329 these cells by dispersing localized cholesterol using the drug 2-hydroxypropyl-β-
330 cyclodextrin. However, this phenotype was not reproducible in *Ae. albopictus*-derived
331 cells, *Aa23*, infected with another supergroup A antiviral *Wolbachia* strain, *w*Au [86,87].
332 Therefore, assessment of all antiviral strains using a common approach will be
333 important in the future to determine whether some antiviral strains utilize different
334 antiviral mechanisms in *Ae. aegypti*.
335 Meanwhile, Manokaran and colleagues discovered that acyl-carnitines
336 (intermediate molecules that transport activated fatty acids, FA-CoA, from the
337 cytoplasm to the mitochondria) are downregulated in the presence of *w*Mel, re-
338 directing lipid sources from β-oxidation, and negatively affecting ATP production,
339 which is required for efficient DENV-1 and Zika virus replication [48]. All these findings
340 support our hypothesis that antiviral *Wolbachia* strains relocalize essential lipid
341 classes and limit their availability to sustain DENV replication.
342 C75 inhibition of LD formation has previously been shown to impact DENV-2
343 RNA amplification in the absence of *Wolbachia*. This is thought to be because C75
344 inhibits association of the capsid protein with host LDs [67,88]. Here, C75 treatment of
345 *w*Mel-*Aag2* cells abrogated LD formation and instead supported an increase in
346 intracellular and infectious titers of DENV-2, to levels comparable with C75-treated
347 *Wolbachia*-free-*Aag2* cells. This partial restoration of DENV-2 replication in *w*Mel-
348 *Aag2*s is consistent with excess LD's induced by *w*Mel having an antiviral role, while
349 also supporting a pro-viral role for moderate levels of LDs [67,88]. That is, complete

350 abrogation of LD formation as we observed in both *w*Mel- and *Wolbachia*-free *Aag2*
351 cells treated with C75, is partially restrictive to DENV.

352 It is important to acknowledge that the C75 target, FAS, does not directly drive
353 formation of LDs, and instead catalysis synthesis of triacylglycerols. Excess free fatty
354 acids are converted into neutral lipids and stored in cytosolic LDs. Primarily, FAS
355 synthesizes palmitate from acetyl-CoA and malonyl-CoA in the presence of NADPH
356 [72]. Thus, although FAS inhibition was associated with reduced LD formation, we
357 cannot exclude the possibility that other FAS-mediated changes in fatty acid
358 homeostasis are responsible for the partial restoration of DENV-2 replication in
359 *w*Mel-*Aag2* cells.

360 One impact of reducing LD formation is the accumulation of lipids at ER
361 membranes, especially precursors of triacylglycerols and sterol esters (such as
362 cholesterol), which constitute most of the structural core of LDs [89,90]. Within the
363 several classes of lipids, sphingolipids and sterols are essential in determining
364 membrane flexibility and stability [91,92]. Therefore, an adequate membrane-lipid
365 composition in the ER is critical for membrane rearrangement and assembly and
366 function of +RNA virus replication complexes [32,33,35,36,61]. Thus, reduction of LD
367 formation following C75 treatment might facilitate DENV-2 acquisition of lipid classes
368 in the ER that may not normally be available in the presence of antiviral *Wolbachia*
369 strains. Moreover, dysregulation of LDs could modify not only the composition of the
370 ER membranes but also the composition of the LDs, both of which are required for
371 DENV replication. In reality, *Wolbachia*'s redistribution of lipids within cells may mask
372 intracellular competition for lipids. That is, differential localization of specific lipid
373 classes that prevent effective viral replication on ER membranes may not have been
374 detected in past lipidomic studies if the overall prevalence of each lipid class remains

375 the same [48,70]. The mechanism by which antiviral *Wolbachia* strains remove lipids
376 from ER membranes and store them as LDs must therefore be further examined.
377 These results provide the first detailed analyses of how antiviral *Wolbachia*
378 strains associate with and modify *Ae. aegypti* cell organelles to restrict viral
379 replication. We identify two striking phenotypes induced only by antiviral strains,
380 including intimate association with host ER membranes, and induction of bigger
381 and/or more numerous LDs. Our data support a role for *Wolbachia*-induced lipid
382 redistribution in restriction of DENV-2 replication.
383

384 **MATERIAL & METHODS**

385 **Cell line generation and maintenance**

386 *w*Mel-*Aedes aegypti*-derived *(Aag2*) cell line and the *Wolbachia*-free
387 *w*Mel.Tet-*Aag2* cell lines have been described previously [56]. Briefly, *w*Mel.Tet-*Aag2*
388 was generated by treating *w*Mel-*Aag2* cell line with 10 µg/mL tetracycline for 3
389 successive passages, to cure the line of *w*Mel infection. This *Wolbachia*-free-*Aag2*
390 cell line was then further used to generate *w*AlbB-*Aag2* and *w*Pip-*Aag2* cell lines.
391 *w*AlbB strain was purified from the *Ae. albopictus*-derived cell line, RML-12, stably
392 infected with *w*AlbB and infection of *Wolbachia*-free-*Aag2* cells was done using the
393 shell vial technique as described previously [59].

394 To generate *w*Pip-*Aag2*, *w*Pip was extracted from infected *Ae. aegypti* eggs
395 [93]. In an Eppendorf tube, 1000-2000 2-5-day old eggs were rinsed 3-5 times in 1mL
396 distilled water. The eggs were passed through a 100 µm mesh sieve and placed in a
397 new Eppendorf tube containing 1 mL 80% v/v ethanol. Eggs were sterilized by 3-5
398 washes in 80% v/v ethanol then rinsed three times in distilled water, sieved, and

399 transferred to a new Eppendorf tube containing 500 µL SPG buffer (218 mM
400 sucrose, 3.8 mM KH_2PO_4, 7.2 mM K_2HPO_4, 4.9 mM L- glutamate at pH 7.4). Eggs
401 were rinsed three times in SPG buffer then homogenized in 300-500 µL SPG buffer
402 using a plastic pestle. The homogenate was spun to remove debris, and the
403 supernatant was collected in a fresh tube. This was repeated three to five times until
404 the supernatant became clear. A pool of supernatant samples was created. Under
405 sterile conditions, the *w*Pip-containing supernatant was then passed through a 5 µm
406 syringe filter followed by a 2.7 µm syringe filter. The filtrate was then centrifuged at
407 12,000 g to pellet *Wolbachia*. Extracted *w*Pip pellet was finally resuspended in ~300
408 µL of sterile SPG buffer. *Wolbachia*-free-*Aag2* cell line was then infected with the
409 purified *w*Pip using the shell vial technique [59].

410 All *Aag2* cell lines (hereafter referred as *Wolbachia*-free-*Aag2*, *w*Mel-*Aag2*,
411 *w*AlbB-*Aag2*, and *w*Pip-*Aag2* cell lines) were routinely cultured at 26°C in
412 maintenance media consisting in 1:1 Schneider's Drosophila (Gibco)/Mitsuhashi and
413 Maramorosch ($CaCl_2$ 0.151 g/L, $MgCl_2$ 0.047 g/L, KCl 0.2 g/L, NaCl 7 g/L, NaH_2PO_4
414 0.174 g/L, D(+)-glucose 4g/L, Yeast extract 5 g/L, Lactalbumin hydrolysate 6.5 g/L,
415 and $NaHCO_3$ 0.12g/L at pH 6.9) medium supplemented with 10% fetal bovine serum
416 (FBS – Gibco).

417 C6/36 cell lines of *Aedes albopictus* origin were supplied by the American
418 Type Culture Collection (ATCC) were routinely cultured at 28°C with 5% CO_2 in
419 RPMI 1640 medium (Gibco) with GlutaMAX™ Supplement containing 10% FBS.

420 ***Wolbachia* Density**

421 *Wolbachia* density was routinely monitored in each cell line. To determine the
422 average number of *Wolbachia* per cell we used qPCR to measure the relative
423 abundance of the conserved *Wolbachia 16S rRNA* gene to that of the single-copy
424 mosquito house-keeping gene *RPS17* gene. *Wolbachia*-free cells and *w*Mel-, *w*AlbB-
425 and *w*Pip-*Aag2* cell lines were lysed with squash extraction buffer (10 mM Tris
426 Buffer, 1 mM ethylenediamine tetraacetic acid [EDTA], 50 mM NaCl in ultrapure
427 water, 1:50 Proteinase K). Cell lysates were then incubated at 56 °C for 5 min,
428 followed by 98 °C for 5 min. Samples were diluted 1:10 in water and qPCR was
429 performed with 3 µL of each diluted cell lysate using the LightCycler 480 Probes
430 Master mix (Roche), according to the manufacturer's instructions. Probes and
431 primers used are as described: For *Wolbachia* detection, *16S rRNA* F (5'-
432 GAGTGAAGAAGG CCTTTGGG-3'), *16S rRNA* R (5'-
433 CACGGAGTTAGCCAGGACTTC-3'), and *16S rRNA* Cy5 probe (5'-
434 LC640CTGTGAGTACCGTCATTATCTTCCTCACT-IowaBlackRQ-3') were used. To
435 detect the housekeeping gene, *RPS17* F (5′-TCCGTGGTATCTCCATCAAGCT-3′),
436 *RPS17* R (5′-CACTTCCGGCACGTAGTTGTC-3′), and *RPS17* FAM probe (5'FAM-
437 CAGGAGGAGGAACGTGAGCGCAG-BHQ1-3') were utilized. PCR cycling
438 conditions were 95 °C for 5 minutes, 45 cycles of 95 °C for 10 seconds, 60 °C for 15
439 seconds, 72 °C for 1 second, followed by cooling at 40 °C for 10 seconds. *Wolbachia*
440 densities were quantified using the delta CT method ($2^{CT(reference)}$/ $2^{CT(target)}$) [94].

441 **DENV-2**

442 Dengue virus serotype 2 (DENV-2) strain 92T (isolated from human serum
443 collected from a patient from Townsville, Queensland/Australia, in 1992) [13] was
444 prepared by inoculation of C6/36 cell lines with a multiplicity of infection (MOI) of 0.1

445 and collection of culture supernatant 13-14 days post-infection. Infectious titers were
446 determined by $TCID_{50}$.

447 **DENV-2 infection of cell lines**

448 *Aag2* cell lines were seeded to reach 90% confluency in 24, 12 or 6 well-plates
449 and incubated at 26°C for 48 hours prior to viral infection. Unless otherwise stated,
450 cells were infected with DENV-2 at MOI 1 in maintenance medium without FBS for 2
451 hours at 26°C. Virus inoculum was then removed and the cells washed once with
452 warm PBS. Maintenance media containing 2% FBS was added and cells were then
453 incubated at 26°C for the indicated time.

454 **Quantification of DENV-2 RNA**

455 To quantify DENV-2 genomic copies, total RNA from virus-infected cells was
456 extracted using the RNeasy kit (Qiagen) or Isolate II RNA mini kit (Bioline). DENV-2
457 RNA was amplified by qRT-PCR (LightCycler Multiplex RNA Virus Master, Roche),
458 using primers to the conserved 3'UTR: Forward 5'-
459 AAGGACTAGAGGTTAGAGGAGACCC; Reverse 5'- CGTTCTGTGCC
460 TGGAATGATG; Probe 5'-HEX- AACAGCATATTGACGCTGGGAGAGACCAGA-
461 BHQ13' [23]; DENV-2 RNA copies were quantified relative to *Ae. aegypti* house-
462 keeping gene *RPS17* (primers and probe sequences as above) using the delta CT
463 method ($2^{CT(reference)}$/ $2^{CT(target)}$) [94]. Reactions were run on a LightCycler 480 (Roche),
464 and data analysis was carried out with the LightCycler 480 software. qRT-PCR
465 conditions: 50 °C for 10 min, 95 °C for 30 s, followed by 45 cycles of 95 °C for 10 s,
466 55 °C for 5 s, and 72 °C for 10 s.

467 **$TCID_{50}$ ELISAs to determine viral titres**

468 Infectious virus levels were determined by $TCID_{50}$ as previously described [95].
469 Briefly, serial dilutions (10-fold) of virus were inoculated onto C6/36 cell lines in flat-

470 bottom 96 well plates containing maintenance medium (RPMI-1640, 2% FBS), and
471 incubated for 13-14 days at 28 °C. After the incubation period, media was aspirated,
472 and cells were fixed with acetone fixative buffer (20% acetone/0.02% BSA in PBS) at
473 4 °C for 24 hours. The fixative was removed and the plate was left to completely air-
474 dry. Once dried, virus concentrations were immediately quantified by ELISA or plates
475 were kept at –20°C until required.
476 ELISAs were performed using monoclonal antibody 4G2 to detect DENV E protein
477 [96]. Briefly, plates were blocked with 2% casein in TNE buffer (10mM Tris; 0.2M NaCl;
478 1mM EDTA; 0.05% Tween20) for 1 hour at room temperature. 4G2 (produced as
479 hybridoma supernatant) [97] was diluted 1:200 in blocking solution and incubated on
480 fixed cells for 1 hour at 37°C. Plates were washed four times with PBST (0.05%
481 Tween20). Anti-mouse secondary antibody was diluted 1:2000 in blocking solution
482 and incubated for 1 hour at 37°C. Plates were washed six times with PBST, then
483 incubated with 3,3'5,5'-Tetramethylbenzidine (TMB) for up to 5 minutes. The reaction
484 was stopped by addition of 0.1M HCl. The absorbance of each well was measured at
485 450nm using a BioTek Gen5 microplate reader (Agilent, Santa Clara, CA, USA). The
486 $TCID_{50}$/ml was determined using the Reed-Muench calculation [98].

487 **Cell fixation and processing for transmission electron microscopy**

488 *Aag2* cell lines were seeded in a 6-well cell culture plate in triplicate at a
489 concentration of 3 x 10^6 cells/well for 48 hours at 26 °C. Unless otherwise stated,
490 cells were mock-infected or infected for 2 hours at 26°C with DENV-2 at MOI 2 in
491 maintenance media without FBS. Virus inoculum was then removed and cells were
492 washed once with warm PBS. Maintenance media containing 2% FBS was added
493 and cells were incubated at 26 °C for 2 days. For C75 treatment, cells were treated
494 as described below and infected with DENV-2 at MOI 1. At 24 hours post-infection,

495 cells were washed once with warm PBS and fixed for 2 hours at room temperature
496 with 2% glutaraldehyde in 0.1 M sodium cacodylate buffer. Cells were gently washed
497 three times for ten minutes each with 0.1 M sodium cacodylate buffer.

498 Cells were post fixed in 1% osmium tetroxide in 0.1M sodium cacodylate
499 buffer for 30 minutes at room temperature which was then reduced with 1.5%
500 potassium ferrocyanide in 0.1M sodium cacodylate buffer for 30 minutes. Cells were
501 washed three times for 10 minutes with ultrapure water. Staining with 2.5% uranyl
502 acetate (aqueous) followed overnight at 4°C. Cells were once again washed three
503 times for 10 minutes with ultrapure water. Following washing, cells were scraped and
504 pelleted into 4% agarose in water. Pellets were dehydrated with increasing
505 concentrations of ethanol (25%, 50%, 75%, 90%, 100%, 100%) followed by acetone
506 (100%, 100%). Each dehydration step was aided by a microwave regime of 40
507 seconds at 150 watts (Pelco Biowave). Pellets were infiltrated with epon resin using
508 a microwave regime (25%, 50%, 75%, 100%, 100%; each step 3 minutes at 250
509 watts under vacuum). Pellets were transfer to fresh 100% epon and left at room
510 temperature overnight and finally embedded in a silicone mold for polymersation for
511 48 hours at 60°C.

512 **Transmission electron microscopy**

513 70nm sections were cut on a ultramicrotome (Leica UC7) and collected on
514 copper mesh grids. Transmission electron microscopy (TEM) imaging was
515 conducted on a Jeol JEM1400-Plus at 80kV. A combination of single snapshots and
516 image montages were acquired, montages were automatically stitched by Jeol
517 acquisition software (TEM Centre).

518 **Electron tomography**

519 200nm sections were collected on copper mesh grids for electron
520 tomography. 10nm gold fiducials were added to both sides of the section. Single axis
521 tomography was performed on a Jeol JEM1400-Plus at 120kV using Jeol Recorder
522 software. Tilt series were recorded with tilt angles from + 65° to − 65° with varying tilt
523 increments based on a Saxton scheme. IMOD software [99] was used to reconstruct
524 tilt series (etomo package), manual segmentation and visualisation.

525 **Immunofluorescence analyses**

526 **Live experiments:** Cells were plated on 18 mm x 18 mm coverslips in a 6-well
527 cell culture plate 48 hours previously coated with gelatin (0.2% [v/v]) [63,84]. To stain
528 the ER, the cell culture medium was aspirated, cells washed with PBS once and
529 incubated for 30 minutes at 26˚C with 1 µM live ER-tracker red dye (Molecular
530 Probes) diluted in the appropriate *Aag2* cell culture medium. The ER-tracker solution
531 was replaced by a 1/20 000 solution of SYTO-11 (Molecular Probes) DNA dye for 10
532 minutes at 26˚C diluted in the appropriate *Aag2* cell culture medium, washed twice
533 with PBS and cells were maintained in *Aag2* culture medium during the confocal
534 microscopy observations.

535 **LDs staining and quantification:** Cells were plated on 12 mm x 12 mm
536 coverslips in a 12-well cell culture plate for 48 hours previously coated with gelatin
537 (0.2% [v/v]) [63,84]. All cells were maintained in *Aag2* cell culture medium with 10%
538 FBS. 24 hours post-DENV-2-infection, mock-infected and infected cells were fixed
539 with 4% paraformaldehyde in PBS for 15 minutes, washed twice with PBS and
540 permeabilized with 0.5% Saponin in PBS for 10 minutes and washed three times
541 with PBS. Cells were blocked with 5% BSA for 1 hour, before antibody staining with
542 polyclonal anti-WSP [96] and 4G2 hybridoma fluid against flavivirus group E antigen for

543 DENV-2 staining. Cells were then incubated with Alexa Fluor 555 or 647 secondary
544 antibodies (1:2000) for 1 hour. LDs were stained by incubating cells with BODIPY
545 (493/503 4,4-difluoro 1,3,5,7,8 pentamethyl 4-bora3a,4a-diaza-s-indacene –
546 Molecular Probes) at 1 ng/mL for 1 hour and nuclei were stained with DAPI (Sigma-
547 Aldrich, 1 µg/ml) for 5 min. All incubations were at room temperature. Samples were
548 then washed with PBS and mounted with Vectashield Antifade Mounting Medium
549 (Vector Laboratories). The slides were imaged as 3-dimensional z-stacks and 2D
550 images generated by Maximum Intensity Projection (MIP). For each condition, at
551 least 6 fields of view were imaged at 63X magnification from different locations
552 across each coverslip. LDs from at least 80 cells per biological replicate with a
553 minimum of 2 biological replicates per experiment being analyzed for both LD
554 number and average LD size. LD numbers and diameters were analyzed using
555 quantitative data from the single raw CZI images (from Zen Blue) in ImageJ using
556 the particle analysis tool.

557 For imaging of mosquito tissues, ovaries were dissected from non-blood-fed
558 female mosquitoes 5-7 days post-emergence. Mosquito lines Rockefeller,
559 Rockefeller-*w*Mel, Rockefeller-*w*AlbB and Rockefeller-*w*Pip have been described
560 previously [23]. Ovaries were dissected from 4-5 mosquitoes per line, in PBS, then
561 fixed on poly-lysine coated slides in cold 4% paraformaldehyde/PBS for 15 minutes.
562 Slides were rinsed three times in PBS, then permeabilized in 0.1% Triton X-100 in
563 PBS for 10 minutes. Samples were blocked with 1% BSA for 30 minutes then
564 stained with BODIPY (493/503) at 1 ng/ml for 1hour. Nuclei were stained with DAPI
565 (Sigma-Aldrich, 1 µg/ml) for 5 minutes at room temperature. Samples were washed
566 with PBS and mounted with Vectashield Antifade Mounting Medium (Vector
567 Laboratories). All images were acquired using a Zeiss LSM 800 confocal microscope

568 and processed using Zeiss analysis software (Zen Blue Edition version 10.1.19043,
569 Jena, Germany) and FIJI analysis software. The slides were imaged as 3-
570 dimensional z-stacks and 2D images generated by MIP.

571 **Inhibition of FAS by C75 treatment**

572 Unless otherwise stated, *Wolbachia*-free and *w*Mel-*Aag2* lines were seeded and
573 infected as described above. Prior to DENV-2 infection cells were pre-treated with 1
574 μM fatty acid synthase (FAS) inhibitor C75 (Abcam) or DMSO diluent only for 24
575 hours. Cells were mock-infected or DENV-2-infected at MOI 1 for 24 hours and C75
576 was maintained during the time of infection in *Aag2* cell culture medium with 10%
577 FBS. LD quantification, viral replication and TEM imaging were performed as
578 described above.

579 **Statistical analyses**

580 Statistical analyses of parametric data were performed using One-way ANOVA or
581 Two-way ANOVA tests with a Tukey's multiple comparison correction, or unpaired
582 two-tailed Student's *t* test, and data were expressed as mean ± Standard Error of the
583 Mean (±SEM). Statistical analyses of non-parametric data were performed using a
584 Kruskal-Wallis test with Dunn's correction for multiple comparisons, or a two-tailed
585 Mann-Whitney test, and data were expressed as median ± Interquartile Range (±
586 IQR). All statistical analyses were performed using Prism 9.3.1 (GraphPad
587 Software), with $p < 0.05$ considered to be significant.

588 **Acknowledgements**

589 This research was funded by the Australian Research Council (DP220102997) and
590 the National Health and Medical Research Council (APP1182432). The funders had
591 no role in study design, data collection and interpretation, or the decision to submit
592 the work for publication.

593 We thank Professor Roy Hall and Jody Hobson-Peters (University of Queensland)
594 for provision of the 4G2 antibody. The authors would like to acknowledge the
595 Ramaciotti Centre for Cryo Electron Microscopy, a node of Microscopy Australia.
596 The authors acknowledge Monash Micro Imaging, Monash University, for the
597 provision of instrumentation, training, and technical support. We would like to thank
598 the La Trobe University Bioimaging Facility for their assistance with image
599 acquisition, data collection, and image analysis essential to this work. Finally, we
600 thank Katrina Ibay for technical support.

601 **Author contributions**

602 R.K.L performed the majority of the experiments; E.A.M assisted in the design of LD
603 experiments, LD imaging and image analyses. R.T. and G.R. assisted with the TEM
604 acquisition. E.A.M and R.T. equally collaborated to this work. J.T.B. originally
605 established all mosquito cell lines and H.F. kindly provided the mosquito lines used
606 in this study. J.M., K.J.H. and C.P.S. assisted in experimental direction. J.E.F. was
607 responsible for the overall study design, alongside R.K.L. J.E.F. and C.P.S. acquired
608 the funding for the project. J.E.F. and R.K.L. wrote the manuscript; all authors
609 contributed to editing of the manuscript.

610 **Competing interests**

611 The authors declare no competing interests.

612

613

614 **FIGURES & LEGENDS:**

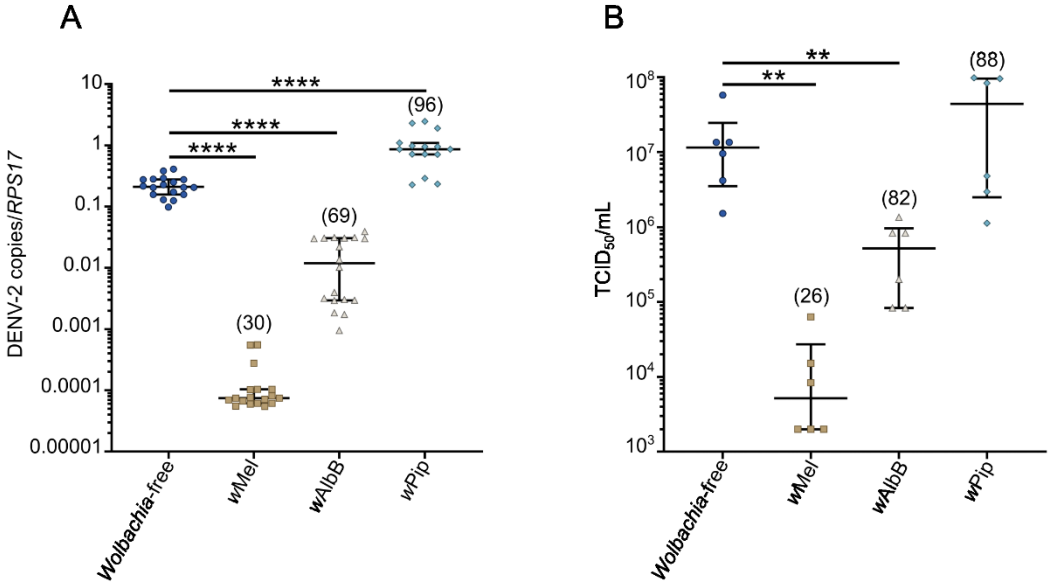

615

616 **Figure 1: *w*Pip does not restrict DENV-2 replication in *Aag2* cells.** *Ae. aegypti*-
617 derived cell lines (*Aag2*) stably infected with *w*Mel, *w*AlbB, and *w*Pip strains were
618 infected with DENV-2 at MOI 1 and compared to their matched *Wolbachia*-free line.
619 Infectious virus and cellular RNA were collected from each cell line 7 days post-
620 infection for analysis by $TCID_{50}$ and qRT-PCR. The numbers in parentheses
621 represent the average number of *Wolbachia* per cell (*Wolbachia 16S rRNA/RPS17*),
622 determined in parallel wells for each independent experiment prior to DENV-2
623 inoculation. (A) Data are the median number of virus genome copies relative to the
624 *RPS17* mosquito housekeeping gene ± IQR. (B) Data are the median infectious viral
625 titres ± IQR determined by $TCID_{50}$. Data are derived from at least 3 (A) or 2 (B)
626 independent experiments performed with triplicate biological replicates each.
627 Statistical analyses were performed using Mann-Whitney test, where ** $p < 0.005$,
628 **** $p < 0.0001$.

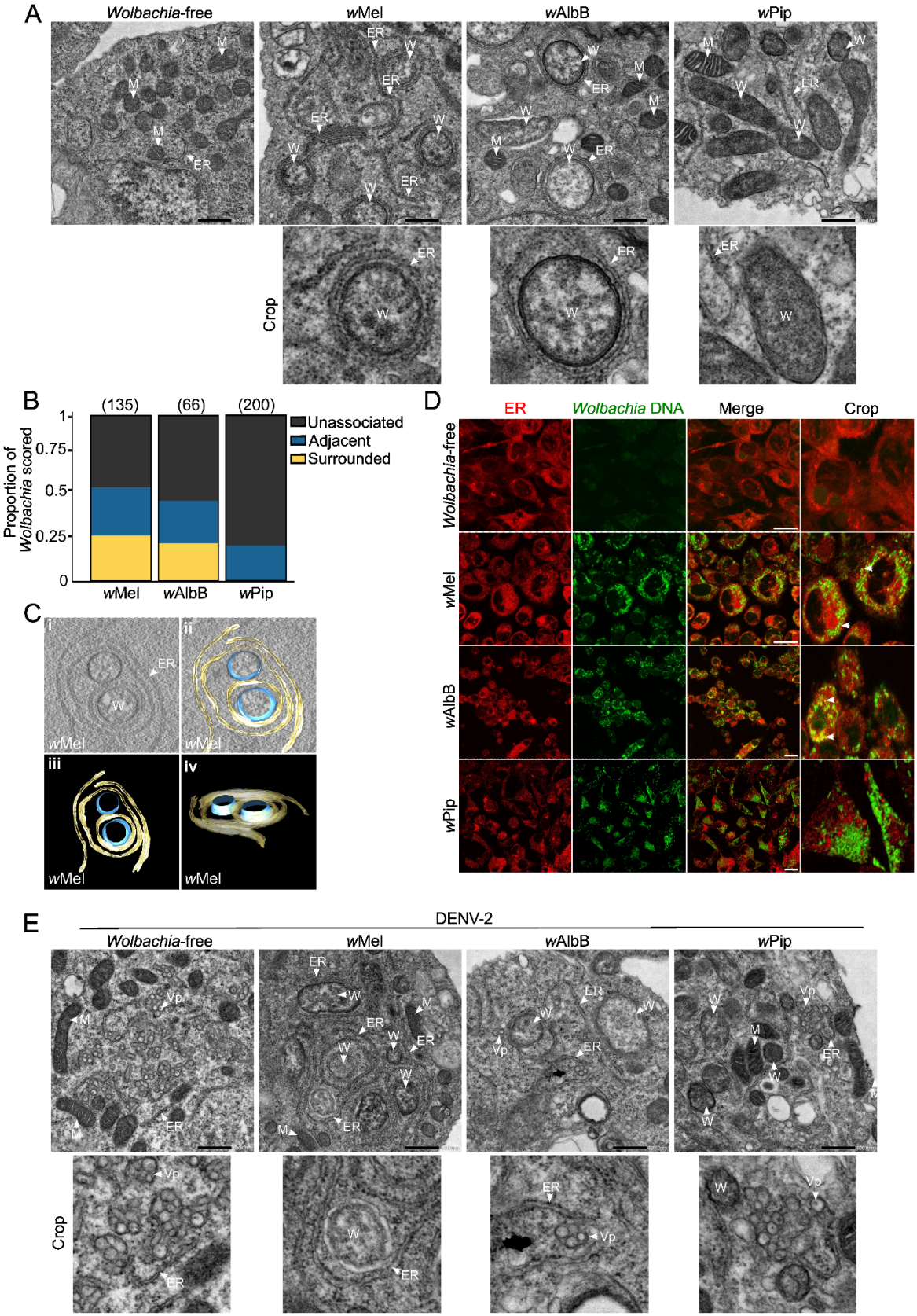

Figure 2: Antiviral *Wolbachia* strains associate with host endoplasmic reticulum membranes. (A) TEM micrographs of *Aag2* cell lines stably infected with *w*Mel, *w*AlbB, and *w*Pip show their intracellular distribution and association with ER

633 membranes. Scale bar = 500nm. (B) *Wolbachia*-ER interactions were manually
634 scored as unassociated, adjacent or surrounded from 2 independent experiments,
635 where *Wolbachia* were counted from a minimum of 28 cells in total per line. The
636 number of *Wolbachia* bacteria scored is in parentheses. (C) TEM tomography shows
637 *w*Mel strain surrounded by ER membranes. See Supplementary Movie 1 for the
638 reconstructed tomogram. (D) Live imaging of all *Aag2* cell lines stained with SYTO
639 11 (*Wolbachia* DNA - green) and ER tracker (red). Scale bar = 15µm. (E) TEM of all
640 *Aag2* cell lines infected with DENV-2 at MOI 2 for 48 hours. Scale bar = 500nm. ER-
641 Endoplasmic reticulum. W- *Wolbachia*. M- Mitochondria. Vp- Vesicle packets.

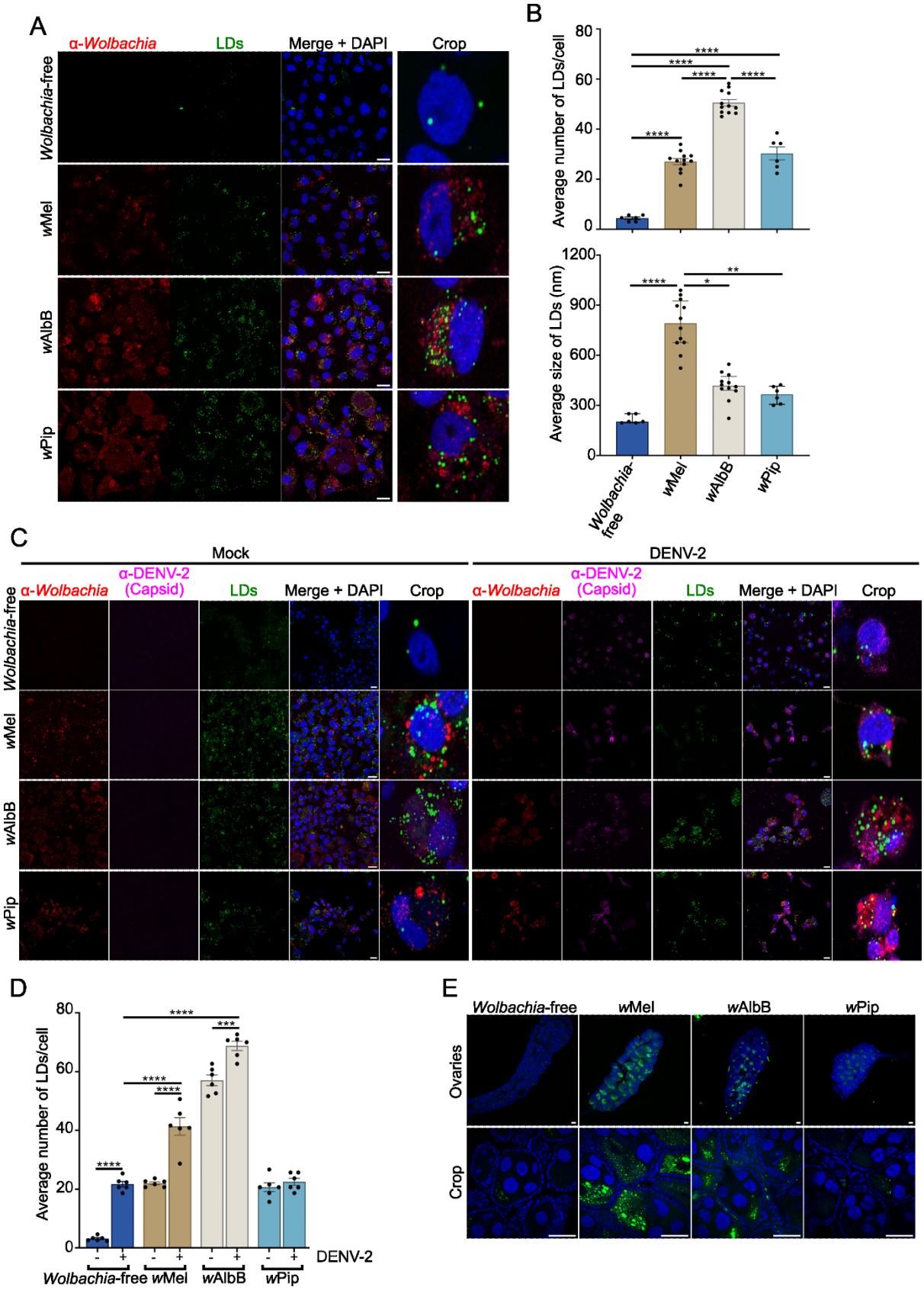

Figure 3: Antiviral *Wolbachia* strains increase lipid droplet formation in mosquito cells. (A-D) *Aag2* cells stably infected with *Wolbachia* strains *w*Mel, *w*AlbB, or *w*Pip, or *Wolbachia*-free cells were mock-infected or DENV-2 infected at MOI 1 for 24 hours. (A and C) All cells were stained with BODIPY (493/503) to

visualize LDs (green) and DAPI to visualize the cell nuclei (blue). *Wolbachia* was detected with an α-WSP antibody (red) and 4G2 hybridoma fluid against flavivirus group E antigen for DENV-2 staining (magenta). Scale bars = 15μm. (B) LD numbers and sizes were analyzed using Fiji software. Data are the mean LD number ±SEM (top) or median LD size ±IQR (bottom) from at least 6 fields of view representing at least 80 cells in total where each data point represents the mean LD number/size from a single field of view. Statistical analyses were performed by One-way ANOVA with Tukey's correction for multiple comparisons (top graph) or Kruskal-Wallis test with Dunn's correction for multiple comparisons (bottom graph). (D) LD numbers were analyzed using Fiji software. Data are the mean LD number ±SEM from at least 6 fields of view representing at least 80 cells in total where each data point represents the mean LD number from a single field of view. Statistical analyses were performed by Two-way ANOVA with Tukey's correction for multiple comparisons, * $p < 0.05$, ** $p < 0.005$, *** $p < 0.0005$, **** $p < 0.0001$. (E) Ovaries were dissected from female mosquitoes 5-7 days post-emergence and stained with BODIPY (green) and DAPI (blue). Scale bars = 50μm. All slides were imaged as 3-dimensional z-stacks and 2D images generated by Maximum Intensity Projection (MIP) using Fiji software.

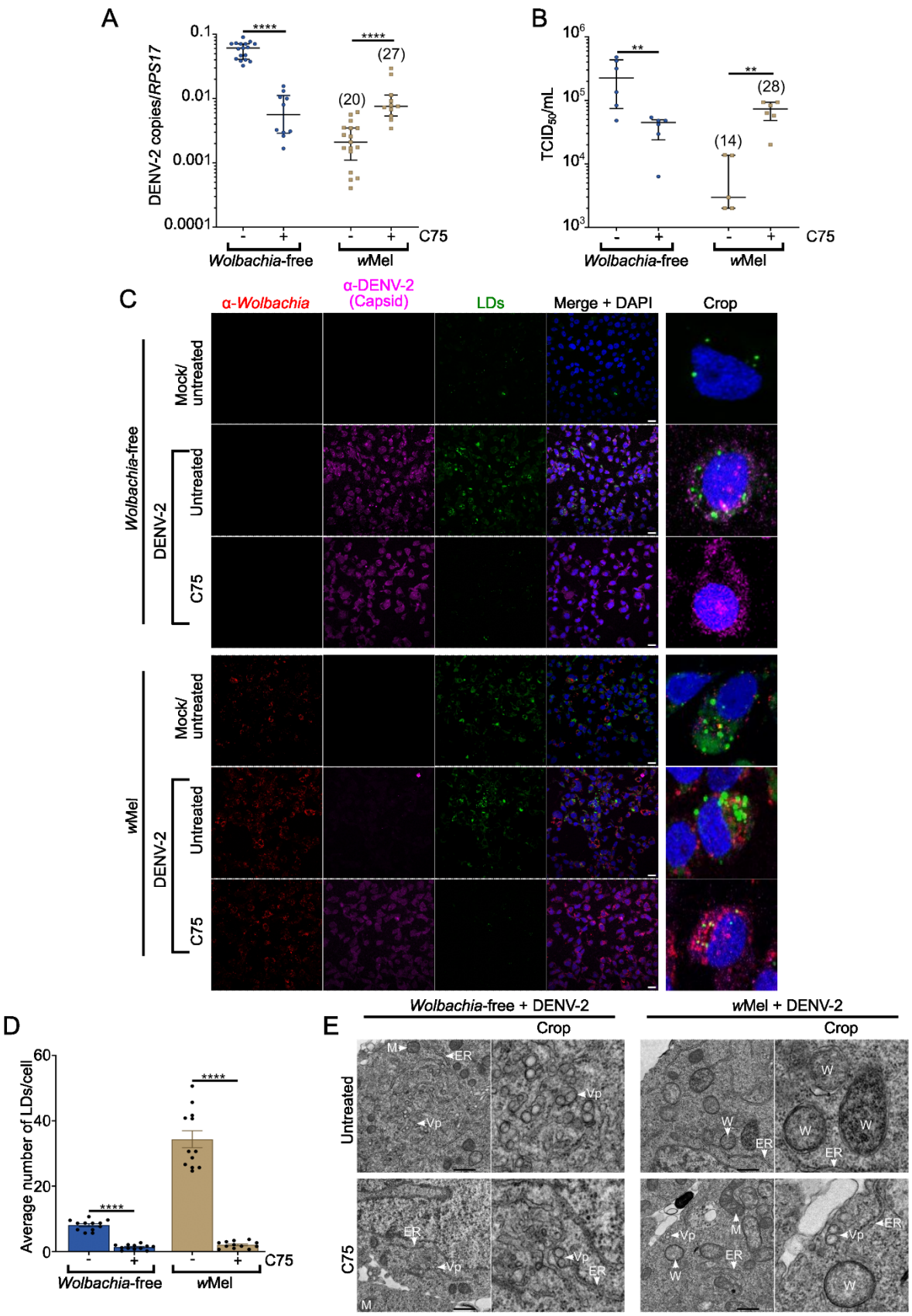

Figure 4. Disrupting *Wolbachia*-induced lipid droplets facilitates viral replication in *w*Mel-*Aag2* cell line. *Wolbachia*-free and *w*Mel-*Aag2* cell lines were mock-infected or DENV-2 infected at MOI 1 for 24 hours. Prior to DENV-2 infection

cells were pre-treated with C75 for 24 hours and C75 was maintained during the time of infection. (A-B) Cell-associated RNA and virus supernatant were collected from each cell line 24 hours post-DENV-2-infection for analysis by qRT-PCR (A) and $TCID_{50}$ (B). Data are the median number of viral genome copies ±IQR relative to the *RPS17* mosquito housekeeping gene (A) or the median $TCID_{50}$/ml ±IQR (B). The numbers in parentheses represent the average number of *Wolbachia* per cell (*Wolbachia 16S rRNA/RPS17*), determined in parallel wells for each independent experiment prior to DENV-2 inoculation. Data are representative of at least 3 (A) or 2 independent experiments (B) with triplicate biological replicates each. Statistical analyses were performed using Mann-Whitney test, where ** $p < 0.001$ and **** $p < 0.0001$. (C) *Wolbachia*-free (top panel) and *w*Mel-*Aag2* cell lines (bottom panel) were stained with BODIPY (green) and DAPI (blue). *Wolbachia* was detected with an α-WSP antibody (red) and an 4G2 hybridoma fluid against flavivirus group E antigen for DENV-2 staining (magenta). Slides were imaged as 3-dimensional z-stacks and 2D images generated by MIP using Fiji software. Scale bars = 15μm. (D) LD numbers were quantified after 24 hours post-DENV-2 infection at MOI 1. LD numbers were analyzed using Fiji software. Data are the mean LD number ±SEM from at least 6 fields of view representing at least 80 cells in total, where each data point represents the mean LD number from a single field of view. Statistical analyses were performed by an unpaired two-tailed Student's *t*-test, where **** $p < 0.0001$. (E) TEM of *Wolbachia*-free and *w*Mel-*Aag2* cell lines mock-infected or DENV-2 infected at MOI 1 for 24 hours and treated with C75 as previously described. Scale bar = 500nm. ER- Endoplasmic reticulum. W- *Wolbachia*. M- Mitochondria. Vp- Vesicle packets.

720 **REFERENCES**

721 1 Ogunlade, S. T. *et al.* A Review: Aedes-Borne Arboviral Infections, Controls and
722 Wolbachia-Based Strategies. *Vaccines* **9**, 32, doi:10.3390/vaccines9010032 (2021).
723 2 Weaver, S. C. & Barrett, A. D. T. Transmission cycles, host range, evolution and
724 emergence of arboviral disease. *Nature Reviews Microbiology* **2**, 789-801,
725 doi:10.1038/nrmicro1006 (2004).
726 3 Mukhopadhyay, S., Kuhn, R. J. & Rossmann, M. G. A structural perspective of the
727 flavivirus life cycle. *Nature Reviews Microbiology* **3**, 13-22, doi:10.1038/nrmicro1067
728 (2005).
729 4 Kraemer, M. U. G. *et al.* Past and future spread of the arbovirus vectors Aedes aegypti
730 and Aedes albopictus. *Nature Microbiology* **4**, 854-863, doi:10.1038/s41564-019-
731 0376-y (2019).
732 5 Brady, O. J. *et al.* Global temperature constraints on Aedes aegypti and Ae. albopictus
733 persistence and competence for dengue virus transmission. *Parasites & Vectors* **7**,
734 338, doi:10.1186/1756-3305-7-338 (2014).
735 6 Ryan, S. J., Carlson, C. J., Mordecai, E. A. & Johnson, L. R. Global expansion and
736 redistribution of Aedes-borne virus transmission risk with climate change. *PLOS*
737 *Neglected Tropical Diseases* **13**, e0007213, doi:10.1371/journal.pntd.0007213 (2019).
738 7 Goindin, D., Delannay, C., Ramdini, C., Gustave, J. & Fouque, F. Parity and Longevity
739 of Aedes aegypti According to Temperatures in Controlled Conditions and
740 Consequences on Dengue Transmission Risks. *PLOS ONE* **10**, e0135489,
741 doi:10.1371/journal.pone.0135489 (2015).
742 8 Morens, D. M., Folkers, G. K. & Fauci, A. S. The challenge of emerging and re-
743 emerging infectious diseases. *Nature* **430**, 242-249, doi:10.1038/nature02759 (2004).
744 9 Kraemer, M. U. G. *et al.* The global compendium of Aedes aegypti and Ae. albopictus
745 occurrence. *Scientific Data* **2**, 150035, doi:10.1038/sdata.2015.35 (2015).
746 10 Liu-Helmersson, J. *et al.* Climate Change and Aedes Vectors: 21st Century Projections
747 for Dengue Transmission in Europe. *EBioMedicine* **7**, 267-277,
748 doi:10.1016/j.ebiom.2016.03.046 (2016).
749 11 Morales, D. *et al.* Resistance Status of Aedes aegypti to Deltamethrin, Malathion, and
750 Temephos in Ecuador. *Journal of the American Mosquito Control Association.* **35**, 113-
751 122, doi:10.2987/19-6831.1info:doi/10.2987/19-6831.1 (2019).
752 12 Bhatt, S. *et al.* The global distribution and burden of dengue. *Nature* **496**, 504-507,
753 doi:10.1038/nature12060 (2013).
754 13 Moreira, L. A. *et al.* A Wolbachia Symbiont in Aedes aegypti Limits Infection with
755 Dengue, Chikungunya, and Plasmodium. *Cell* **139**, 1268-1278,
756 doi:10.1016/j.cell.2009.11.042 (2009).
757 14 Walker, T. *et al.* The wMel Wolbachia strain blocks dengue and invades caged Aedes
758 aegypti populations. *Nature* **476**, 450-453, doi:10.1038/nature10355 (2011).
759 15 Bian, G., Xu, Y., Lu, P., Xie, Y. & Xi, Z. The Endosymbiotic Bacterium Wolbachia
760 Induces Resistance to Dengue Virus in Aedes aegypti. *PLoS Pathogens* **6**, e1000833,
761 doi:10.1371/journal.ppat.1000833 (2010).
762 16 Carrington, L. B. *et al.* Field- and clinically derived estimates of Wolbachia-mediated
763 blocking of dengue virus transmission potential in Aedes aegypti mosquitoes.
764 *Proceedings of the National Academy of Sciences* **115**, 361-366,
765 doi:10.1073/pnas.1715788115 (2018).
766 17 Aliota, M. T. *et al.* The wMel Strain of Wolbachia Reduces Transmission of
767 Chikungunya Virus in Aedes aegypti. *PLOS Neglected Tropical Diseases* **10**,
768 e0004677, doi:10.1371/journal.pntd.0004677 (2016).
769 18 Zug, R. & Hammerstein, P. Still a Host of Hosts for Wolbachia: Analysis of Recent Data
770 Suggests That 40% of Terrestrial Arthropod Species Are Infected. *PLoS ONE* **7**,
771 e38544, doi:10.1371/journal.pone.0038544 (2012).

19 Ross, P. A. *et al.* An elusive endosymbiont: Does Wolbachia occur naturally in Aedes aegypti? *Ecology and Evolution* **10**, 1581-1591, doi:10.1002/ece3.6012 (2020).
20 Ant, T. H., Herd, C. S., Geoghegan, V., Hoffmann, A. A. & Sinkins, S. P. The Wolbachia strain wAu provides highly efficient virus transmission blocking in Aedes aegypti. *PLOS Pathogens* **14**, e1006815, doi:10.1371/journal.ppat.1006815 (2018).
21 Xi, Z., Khoo, C. C. H. & Dobson, S. L. Wolbachia Establishment and Invasion in an Aedes aegypti Laboratory Population. *Science.* **310**, 326-328, doi:10.1126/science.1117607info:doi/10.1126/science.1117607 (2005).
22 Flores, H. A. *et al.* Multiple Wolbachia strains provide comparative levels of protection against dengue virus infection in Aedes aegypti. *PLOS Pathogens* **16**, e1008433, doi:10.1371/journal.ppat.1008433 (2020).
23 Fraser, J. E. *et al.* Novel phenotype of Wolbachia strain wPip in Aedes aegypti challenges assumptions on mechanisms of Wolbachia-mediated dengue virus inhibition. *PLOS Pathogens* **16**, e1008410, doi:10.1371/journal.ppat.1008410 (2020).
24 Sinkins, S. P., Braig, H. R. & O'Neill, S. L. Wolbachia superinfections and the expression of cytoplasmic incompatibility. *Proceedings of the Royal Society of London. Series B: Biological Sciences* **261**, 325-330, doi:10.1098/rspb.1995.0154 (1995).
25 Serbus, L. R., Casper-Lindley, C., Landmann, F. & Sullivan, W. The Genetics and Cell Biology of Wolbachia -Host Interactions. *Annual Review of Genetics* **42**, 683-707, doi:10.1146/annurev.genet.41.110306.130354 (2008).
26 Indriani, C. *et al.* Reduced dengue incidence following deployments of Wolbachia-infected Aedes aegypti in Yogyakarta, Indonesia: a quasi-experimental trial using controlled interrupted time series analysis. *Gates Open Research* **4**, 50, doi:10.12688/gatesopenres.13122.1 (2020).
27 Utarini, A. *et al.* Efficacy of Wolbachia-Infected Mosquito Deployments for the Control of Dengue. *New England Journal of Medicine* **384**, 2177-2186, doi:10.1056/nejmoa2030243 (2021).
28 Nazni, W. A. *et al.* Establishment of Wolbachia Strain wAlbB in Malaysian Populations of Aedes aegypti for Dengue Control. *Current Biology* **29**, 4241-4248.e4245, doi:10.1016/j.cub.2019.11.007 (2019).
29 O'Neill, S. L. *et al.* Scaled deployment of Wolbachia to protect the community from dengue and other Aedes transmitted arboviruses. *Gates Open Research* **2**, 36, doi:10.12688/gatesopenres.12844.3 (2019).
30 Ryan, P. A. *et al.* Establishment of wMel Wolbachia in Aedes aegypti mosquitoes and reduction of local dengue transmission in Cairns and surrounding locations in northern Queensland, Australia. *Gates Open Research* **3**, 1547, doi:10.12688/gatesopenres.13061.2 (2020).
31 Pinto, S. B. *et al.* Effectiveness of Wolbachia-infected mosquito deployments in reducing the incidence of dengue and other Aedes-borne diseases in Niteroi, Brazil: A quasi-experimental study. *PLoS Negl Trop Dis* **15**, e0009556, doi:10.1371/journal.pntd.0009556 (2021).
32 Harapan, H., Michie, A., Sasmono, R. T. & Imrie, A. Dengue: A Minireview. *Viruses* **12**, 829, doi:10.3390/v12080829 (2020).
33 Guzman, M. G., Gubler, D. J., Izquierdo, A., Martinez, E. & Halstead, S. B. Dengue infection. *Nature Reviews Disease Primers* **2**, 16055, doi:10.1038/nrdp.2016.55 (2016).
34 Van Den Elsen, K., Quek, J. P. & Luo, D. Molecular Insights into the Flavivirus Replication Complex. *Viruses* **13**, 956, doi:10.3390/v13060956 (2021).
35 Welsch, S. *et al.* Composition and Three-Dimensional Architecture of the Dengue Virus Replication and Assembly Sites. *Cell Host & Microbe* **5**, 365-375, doi:10.1016/j.chom.2009.03.007 (2009).
36 Eyre, N. S. *et al.* Genome-Wide Mutagenesis of Dengue Virus Reveals Plasticity of the NS1 Protein and Enables Generation of Infectious Tagged Reporter Viruses. *J Virol* **91**, doi:10.1128/JVI.01455-17 (2017).

826 37 Lescar, J. *et al.* in *Advances in Experimental Medicine and Biology* 115-129
827 (Springer Singapore, 2018).
828 38 Jason M. Mackenzie, M. K. J., Paul R. Young. Improved membrane preservation of
829 flavivirus-infected cells with cryosectioning. *Journal of Virological Methods* **56**,
830 doi:https://doi.org/10.1016/0166-0934(95)01916-2 (1996).
831 39 Westaway, E. G., Mackenzie, J. M., Kenney, M. T., Jones, M. K. & Khromykh, A. A.
832 Ultrastructure of Kunjin virus-infected cells: colocalization of NS1 and NS3 with double-
833 stranded RNA, and of NS2B with NS3, in virus-induced membrane structures. *Journal*
834 *of Virology* **71**, 6650-6661, doi:10.1128/jvi.71.9.6650-6661.1997 (1997).
835 40 Amuzu, H. E. & Mcgraw, E. A. Wolbachia-Based Dengue Virus Inhibition Is Not Tissue-
836 Specific in Aedes aegypti. *PLOS Neglected Tropical Diseases* **10**, e0005145,
837 doi:10.1371/journal.pntd.0005145 (2016).
838 41 Nainu, F., Trenerry, A. & Johnson, K. N. Wolbachia-mediated antiviral protection is
839 cell-autonomous. *Journal of General Virology* **100**, 1587-1592,
840 doi:10.1099/jgv.0.001342 (2019).
841 42 Thomas, S., Verma, J., Woolfit, M. & O'Neill, S. L. Wolbachia-mediated virus blocking
842 in mosquito cells is dependent on XRN1-mediated viral RNA degradation and
843 influenced by viral replication rate. *PLOS Pathogens* **14**, e1006879,
844 doi:10.1371/journal.ppat.1006879 (2018).
845 43 Bhattacharya, T., Newton, I. L. G. & Hardy, R. W. Viral RNA is a target for Wolbachia-
846 mediated pathogen blocking. *PLOS Pathogens* **16**, e1008513,
847 doi:10.1371/journal.ppat.1008513 (2020).
848 44 Caragata, E. P. *et al.* Dietary Cholesterol Modulates Pathogen Blocking by Wolbachia.
849 *PLoS Pathogens* **9**, e1003459, doi:10.1371/journal.ppat.1003459 (2013).
850 45 Caragata, E. P., Rancès, E., O'Neill, S. L. & Mcgraw, E. A. Competition for Amino
851 Acids Between Wolbachia and the Mosquito Host, Aedes aegypti. *Microbial Ecology*
852 **67**, 205-218, doi:10.1007/s00248-013-0339-4 (2014).
853 46 Cho, K.-O., Kim, G.-W. & Lee, O.-K. Wolbachia Bacteria Reside in Host Golgi-Related
854 Vesicles Whose Position Is Regulated by Polarity Proteins. *PLoS ONE* **6**, e22703,
855 doi:10.1371/journal.pone.0022703 (2011).
856 47 White, P. M. *et al.* Reliance of Wolbachia on High Rates of Host Proteolysis Revealed
857 by a Genome-Wide RNAi Screen of Drosophila Cells. *Genetics* **205**, 1473-1488,
858 doi:10.1534/genetics.116.198903 (2017).
859 48 Manokaran, G. *et al.* Modulation of acyl-carnitines, the broad mechanism behind
860 Wolbachia-mediated inhibition of medically important flaviviruses in Aedes aegypti.
861 *Proceedings of the National Academy of Sciences* **117**, 24475-24483,
862 doi:10.1073/pnas.1914814117 (2020).
863 49 Zhang, G., Hussain, M., O'Neill, S. L. & Asgari, S. Wolbachia uses a host microRNA
864 to regulate transcripts of a methyltransferase, contributing to dengue virus inhibition in
865 Aedes aegypti. *Proceedings of the National Academy of Sciences* **110**, 10276-10281,
866 doi:10.1073/pnas.1303603110 (2013).
867 50 Mayoral, J. G., Etebari, K., Hussain, M., Khromykh, A. A. & Asgari, S. Wolbachia
868 Infection Modifies the Profile, Shuttling and Structure of MicroRNAs in a Mosquito Cell
869 Line. *PLoS ONE* **9**, e96107, doi:10.1371/journal.pone.0096107 (2014).
870 51 Bhattacharya, T. Y., Liewei; Crawford, John M.; Zaher, Hani; Newton, Irene L. G. ;
871 Hardy, Richard W. . Wolbachia and Virus Alter the Host Transcriptome at the Interface
872 of Nucleotide Metabolism Pathways. *mBio* **12**, doi:https://doi.org/10.1128/mbio.03472-
873 20 (2021).
874 52 Bhattacharya, T. *et al.* Differential viral RNA methylation contributes to pathogen
875 blocking in Wolbachia-colonized arthropods. *PLoS Pathog* **18**, e1010393,
876 doi:10.1371/journal.ppat.1010393 (2022).
877 53 Rancès, E., Ye, Y. H., Woolfit, M., McGraw, E. A. & O'Neill, S. L. The relative
878 importance of innate immune priming in Wolbachia-mediated dengue interference.
879 *PLoS Pathog* **8**, e1002548, doi:10.1371/journal.ppat.1002548 (2012).

880 54 Pan, X. *et al. Wolbachia* induces reactive oxygen species (ROS)-dependent activation
881 of the Toll pathway to control dengue virus in the mosquito *Aedes aegypti*. *Proceedings*
882 *of the National Academy of Sciences* **109**, E23-E31, doi:10.1073/pnas.1116932108
883 (2012).
884 55 Fraser, J. E. *et al.* Novel Wolbachia-transinfected Aedes aegypti mosquitoes possess
885 diverse fitness and vector competence phenotypes. *PLOS Pathogens* **13**, e1006751,
886 doi:10.1371/journal.ppat.1006751 (2017).
887 56 McLean, B. J., Dainty, K. R., Flores, H. A. & O'Neill, S. L. Differential suppression of
888 persistent insect specific viruses in trans-infected wMel and wMelPop-CLA Aedes-
889 derived mosquito lines. *Virology.* **527**, 141-145, doi:10.1016/j.virol.2018.11.012

890 info:doi/10.1016/j.virol.2018.11.012 (2019).
891 57 McLean, B. J., Dainty, K. R., Flores, H. A. & O'Neill, S. L. Differential suppression of
892 persistent insect specific viruses in trans-infected wMel and wMelPop-CLA Aedes-
893 derived mosquito lines. *Virology* **527**, 141-145,
894 doi:https://doi.org/10.1016/j.virol.2018.11.012 (2019).
895 58 Fattouh, N., Cazevieille, C. & Landmann, F. Wolbachia endosymbionts subvert the
896 endoplasmic reticulum to acquire host membranes without triggering ER stress. *PLOS*
897 *Neglected Tropical Diseases* **13**, e0007218, doi:10.1371/journal.pntd.0007218 (2019).
898 59 Mcmeniman, C. J. *et al.* Host Adaptation of a Wolbachia Strain after Long-Term Serial
899 Passage in Mosquito Cell Lines. *Applied and Environmental Microbiology* **74**, 6963-
900 6969, doi:10.1128/aem.01038-08 (2008).
901 60 Casper-Lindley, C. *et al.* Rapid fluorescence-based screening for Wolbachia
902 endosymbionts in Drosophila germ line and somatic tissues. *Appl Environ Microbiol*
903 **77**, 4788-4794, doi:10.1128/AEM.00215-11 (2011).
904 61 Harris, E. & Guzman, M. G. Dengue. *The lancet.* **385**, 453-465, doi:10.1016/S0140-
905 6736(14)60572-9info:doi/10.1016/S0140-6736(14)60572-9 (2015).
906 62 Barletta, A. B. F. *et al.* Emerging role of lipid droplets in Aedes aegypti immune
907 response against bacteria and Dengue virus. *Scientific Reports* **6**, 19928,
908 doi:10.1038/srep19928 (2016).
909 63 Monson, E. A. *et al.* Intracellular lipid droplet accumulation occurs early following viral
910 infection and is required for an efficient interferon response. *Nature Communications*
911 **12**, doi:10.1038/s41467-021-24632-5 (2021).
912 64 Olzmann, J. A. & Carvalho, P. Dynamics and functions of lipid droplets. *Nature*
913 *Reviews Molecular Cell Biology* **20**, 137-155, doi:10.1038/s41580-018-0085-z (2019).
914 65 Tang, W. C., Lin, R. J., Liao, C. L. & Lin, Y. L. Rab18 facilitates dengue virus infection
915 by targeting fatty acid synthase to sites of viral replication. *J Virol* **88**, 6793-6804,
916 doi:10.1128/JVI.00045-14 (2014).
917 66 Junjhon, J. *et al.* Ultrastructural characterization and three-dimensional architecture of
918 replication sites in dengue virus-infected mosquito cells. *J Virol* **88**, 4687-4697,
919 doi:10.1128/JVI.00118-14 (2014).
920 67 Samsa, M. M. *et al.* Dengue Virus Capsid Protein Usurps Lipid Droplets for Viral
921 Particle Formation. *PLoS Pathogens* **5**, e1000632, doi:10.1371/journal.ppat.1000632
922 (2009).
923 68 Molloy, J. C., Sommer, U., Viant, M. R. & Sinkins, S. P. Wolbachia Modulates Lipid
924 Metabolism in Aedes albopictus Mosquito Cells. *Appl Environ Microbiol* **82**, 3109-3120,
925 doi:10.1128/aem.00275-16 (2016).
926 69 Ponton, F. *et al.* Macronutrients mediate the functional relationship between
927 *Drosophila* and *Wolbachia*. *Proceedings of the Royal Society B: Biological Sciences*
928 **282**, 20142029, doi:10.1098/rspb.2014.2029 (2015).
929 70 Koh, C. *et al.* Dengue virus dominates lipid metabolism modulations in Wolbachia-
930 coinfected Aedes aegypti. *Commun Biol* **3**, 518, doi:10.1038/s42003-020-01254-z
931 (2020).
932 71 Heier, C. & Kuhnlein, R. P. Triacylglycerol Metabolism in Drosophila melanogaster.
933 *Genetics* **210**, 1163-1184, doi:10.1534/genetics.118.301583 (2018).

72 Chirala, S. S. & Wakil, S. J. Structure and function of animal fatty acid synthase. *Lipids* **39**, 1045-1053, doi:10.1007/s11745-004-1329-9 (2004).
73 *World Health Organization - Thirteenth meeting of the WHO Vector Control Advisory Group*, <https://www.who.int/publications-detail-redirect/9789240021792> (2021).
74 Baldo, L. *et al.* Multilocus Sequence Typing System for the Endosymbiont Wolbachia pipientis. *Applied and Environmental Microbiology* **72**, 7098-7110, doi:10.1128/aem.00731-06 (2006).
75 Landmann, F. The Wolbachia Endosymbionts. *Microbiol Spectr* **7**, doi:10.1128/microbiolspec.BAI-0018-2019 (2019).
76 Wu, M. *et al.* Phylogenomics of the Reproductive Parasite Wolbachia pipientis wMel: A Streamlined Genome Overrun by Mobile Genetic Elements. *PLoS Biology* **2**, e69, doi:10.1371/journal.pbio.0020069 (2004).
77 Ant, T. H., Mancini, M. V., Mcnamara, C. J., Rainey, S. M. & Sinkins, S. P. Wolbachia-Virus interactions and arbovirus control through population replacement in mosquitoes. *Pathogens and Global Health*, 1-14, doi:10.1080/20477724.2022.2117939 (2022).
78 Lin, M. & Rikihisa, Y. *Ehrlichia chaffeensis* and *Anaplasma phagocytophilum* Lack Genes for Lipid A Biosynthesis and Incorporate Cholesterol for Their Survival. *Infection and Immunity* **71**, 5324-5331, doi:10.1128/iai.71.9.5324-5331.2003 (2003).
79 Monson, E. A., Trenerry, A. M., Laws, J. L., Mackenzie, J. M. & Helbig, K. J. Lipid droplets and lipid mediators in viral infection and immunity. *FEMS Microbiology Reviews*, doi:10.1093/femsre/fuaa066 (2021).
80 Heaton, N. S. *et al.* Dengue virus nonstructural protein 3 redistributes fatty acid synthase to sites of viral replication and increases cellular fatty acid synthesis. *Proceedings of the National Academy of Sciences* **107**, 17345-17350, doi:10.1073/pnas.1010811107 (2010).
81 Perera, R. *et al.* Dengue Virus Infection Perturbs Lipid Homeostasis in Infected Mosquito Cells. *PLoS Pathogens* **8**, e1002584, doi:10.1371/journal.ppat.1002584 (2012).
82 Hitakarun, A. *et al.* Cell Type Variability in the Incorporation of Lipids in the Dengue Virus Virion. *Viruses* **14**, 2566, doi:10.3390/v14112566 (2022).
83 Carro, A. C. & Damonte, E. B. Requirement of cholesterol in the viral envelope for dengue virus infection. *Virus Res* **174**, 78-87, doi:10.1016/j.virusres.2013.03.005 (2013).
84 Monson, E. A., Crosse, K. M., Das, M. & Helbig, K. J. Lipid droplet density alters the early innate immune response to viral infection. *PLOS ONE* **13**, e0190597, doi:10.1371/journal.pone.0190597 (2018).
85 Monson, E. A., Whelan, D. R. & Helbig, K. J. Lipid Droplet Motility Increases Following Viral Immune Stimulation. *International Journal of Molecular Sciences* **22**, 4418, doi:10.3390/ijms22094418 (2021).
86 Geoghegan, V. *et al.* Perturbed cholesterol and vesicular trafficking associated with dengue blocking in Wolbachia-infected Aedes aegypti cells. *Nature Communications* **8**, doi:10.1038/s41467-017-00610-8 (2017).
87 Rainey, S. M. *et al.* Differences in proteome perturbations caused by the Wolbachia strain wAu suggest multiple mechanisms of Wolbachia-mediated antiviral activity. *Scientific Reports* **13**, doi:10.1038/s41598-023-38127-4 (2023).
88 Heaton, N. S. & Randall, G. Dengue Virus-Induced Autophagy Regulates Lipid Metabolism. *Cell Host & Microbe* **8**, 422-432, doi:10.1016/j.chom.2010.10.006 (2010).
89 Thiele, C. & Penno, A. Lipid Droplets. *Encyclopedia of Cell Biology*, 273-278, doi:10.1016/B978-0-12-394447-4.20023-0info:doi/10.1016/B978-0-12-394447-4.20023-0 (2016).
90 Gao, M., Huang, X., Song, B.-L. & Yang, H. The biogenesis of lipid droplets: Lipids take center stage. *Progress in lipid research.* **75**, 100989, doi:10.1016/j.plipres.2019.100989info:doi/10.1016/j.plipres.2019.100989 (2019).

91 Zaitseva, E., Yang, S.-T., Melikov, K., Pourmal, S. & Chernomordik, L. V. Dengue Virus Ensures Its Fusion in Late Endosomes Using Compartment-Specific Lipids. *PLoS Pathogens* **6**, e1001131, doi:10.1371/journal.ppat.1001131 (2010).

92 Kielian, M., Chanel-Vos, C. & Liao, M. Alphavirus Entry and Membrane Fusion. *Viruses* **2**, 796-825, doi:10.3390/v2040796 (2010).

93 Fraser, J. E. *et al.* Novel Wolbachia-transinfected Aedes aegypti mosquitoes possess diverse fitness and vector competence phenotypes. *PLoS Pathog* **13**, e1006751, doi:10.1371/journal.ppat.1006751 (2017).

94 Livak, K. J. & Schmittgen, T. D. Analysis of relative gene expression data using real-time quantitative PCR and the 2(-Delta Delta C(T)) Method. *Methods* **25**, 402-408, doi:10.1006/meth.2001.1262 (2001).

95 O'Brien, C. A. *et al.* Viral RNA Intermediates as Targets for Detection and Discovery of Novel and Emerging Mosquito-Borne Viruses. *PLOS Neglected Tropical Diseases* **9**, e0003629, doi:10.1371/journal.pntd.0003629 (2015).

96 Lee, E. *et al.* Transient Introgression of Wolbachia into Aedes aegypti Populations Does Not Elicit an Antibody Response to Wolbachia Surface Protein in Community Members. *Pathogens* **11**, 535, doi:10.3390/pathogens11050535 (2022).

97 McCown, J. M., Dalrymple, J. M., Gentry, M. K., Brandt, W. E. & Henchal, E. A. Identification of Distinct Antigenic Determinants on Dengue-2 Virus Using Monoclonal Antibodies. *The American Journal of Tropical Medicine and Hygiene* **31**, 548-555, doi:10.4269/ajtmh.1982.31.548info:doi/10.4269/ajtmh.1982.31.548 (1982).

98 Reed, L. J. & Muench, H. A simple method of estimating fifty per cent endpoints. *American journal of epidemiology.* **27**, 493-497, doi:10.1093/oxfordjournals.aje.a118408info:doi/10.1093/oxfordjournals.aje.a118408 (1938).

99 JAMES R. KREMER, D. N. M., AND J. RICHARD MCINTOSH. Computer Visualization of Three-Dimensional Image Data Using IMOD. *JOURNAL OF STRUCTURAL BIOLOGY* **116**, 71–76 (1996).

Supplementary information for:

Antiviral *Wolbachia* strains associate with *Aedes aegypti* endoplasmic reticulum membranes and disturb host cell lipid distribution to restrict dengue virus replication

Robson K. Loterio[1], Ebony A. Monson[2*], Rachel Templin[3*], Jyotika T. Bruyne[4], Heather A. Flores[5] Jason M. Mackenzie[6], Georg Ramm[3], Karla J. Helbig[2], Cameron P. Simmons[1,4], Johanna E. Fraser[1#]

[1]Department of Microbiology, Biomedicine Discovery Institute, Monash University, Clayton, Australia; [2]Department of Physiology, Anatomy, and Microbiology, School of Life Sciences, La Trobe University, Melbourne, Australia; [3]Ramaciotti Centre For Cryo-Electron Microscopy, Monash University, Clayton, Australia; [4]World Mosquito Program, Monash University, Clayton, Australia; [5]School of Biological Sciences, Monash University, Clayton, Australia; [6]Department of Microbiology and Immunology, University of Melbourne at the Peter Doherty Institute for Infection and Immunity, Melbourne, Australia. *These authors contributed equally.

Corresponding author: johanna.fraser@monash.edu

This PDF file includes:

Supplementary text information
Supplementary Fig. 1 to Fig.3
SI References

45 **Supplementary text information:**

46 **Extended Material and Methods**

47 **Mosquito rearing**

48 All *Ae*. *aegypti* mosquitoes were reared and maintained as described previously [1].
49 Briefly, adult mosquitoes were maintained at 26˚C, 65% relative humidity, and a 12 h
50 light:dark cycle in a climate-controlled room, and were allowed access to 10%
51 sucrose *ad libitum.* Mosquitoes were blood fed on the arms of human volunteers for
52 reproduction. To generate a panel of genetically comparable *Wolbachia*-carrying *Ae*.
53 *aegypti* lines, we backcrossed females from the *w*Mel, *w*AlbB, and *w*Pip to males of
54 the inbred laboratory *Ae*. *aegypti* line, Rockefeller [2] (BEI resources), for six
55 generations. To exclude any influence of mosquito age on our experiments, age-
56 controlled adults emerging within a 48 hours window were used.

57

58 **Live Lipid Droplet Staining**

59 For live staining of LDs, *Wolbachia*-free and *w*Mel-*Aag2* cell lines were seeded in a
60 96-well black cell culture plate with 6 replicates per condition and at 1 x 10^5
61 cells/well. Cells were incubated for 24 hours at 26 °C with *Aag2* cell culture medium
62 with 10% FBS. After 24 hours, the culture medium was replaced with fresh medium
63 containing DMSO only, 1 μM C75, 2.5 μM DGAT 1 (T863), 10 μM DGAT 2 (PF-
64 06424439) or DGAT 1 and 2 combined, and incubated for another 24 hours. After
65 incubation time, cell culture medium was replaced with 5 μM BODIPY 493/503 in cell
66 culture medium for 1 hour at 26 °C. For each condition, extra wells were designated
67 to not have cells or cells without BODIPY staining for appropriate background
68 reduction. Cells were then gently washed 2 times with warm PBS and cells were
69 maintained in PBS for fluorescence acquisition. Fluorescence was detected with a

microplate reader (BioTek Gen5 - Agilent, Santa Clara, CA, USA) equipped for excitation in the 485/20 nm range and emission detection at 535/20 nm (FITC wavelength).

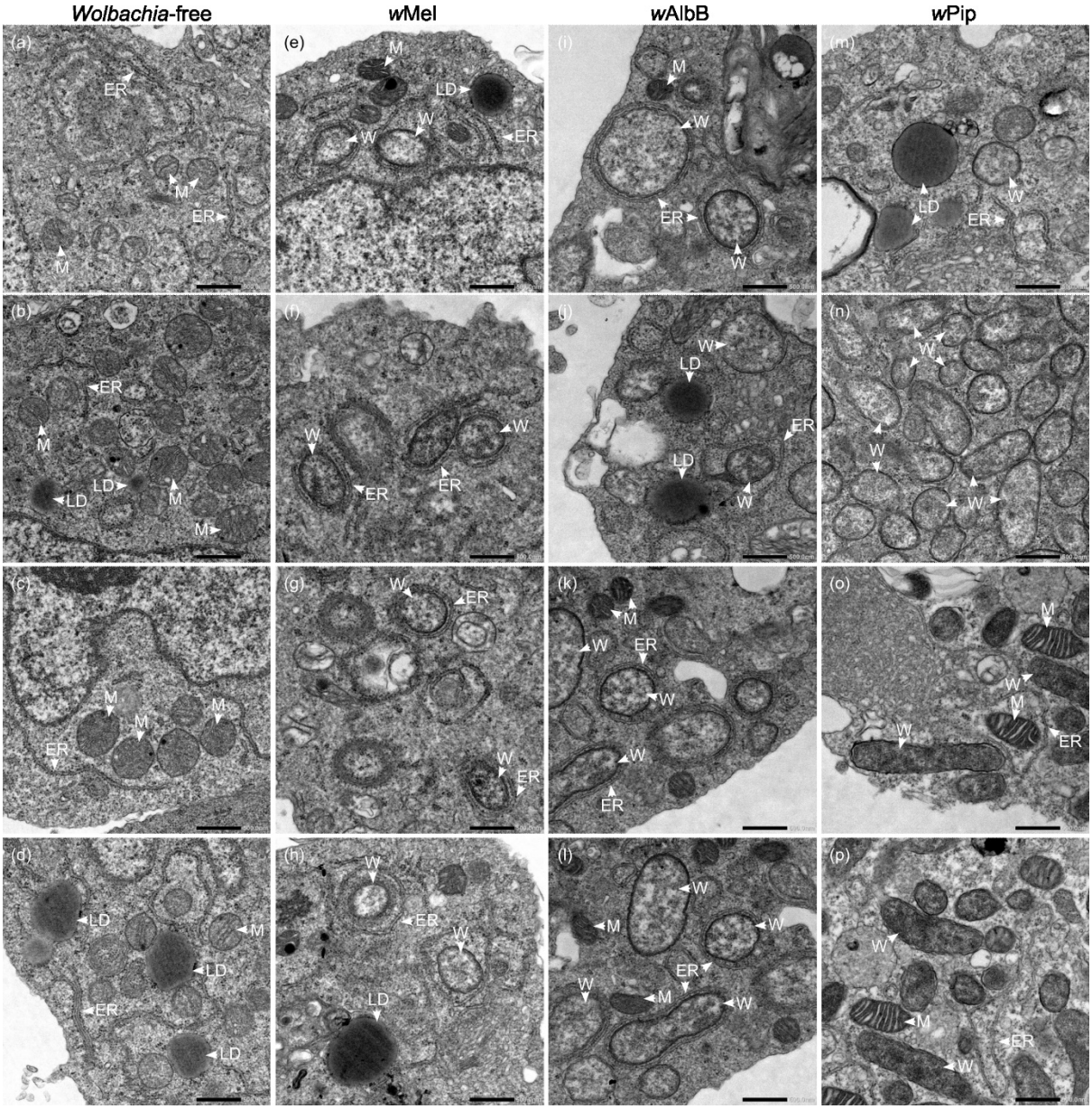

Supplementary Fig. 1: Antiviral *Wolbachia* strains are frequently wrapped by the host endoplasmic reticulum membranes. TEM micrographs of *Wolbachia*-free-*Aag2* cell line (a-d) or stably infected with *w*Mel (e-h), *w*AlbB (i-l), and *w*Pip (m-p) show their intracellular distribution and association with the ER membranes. Scale bar = 500nm. ER- Endoplasmic reticulum. W- *Wolbachia*. M- Mitochondria. LD- Lipid Droplet.

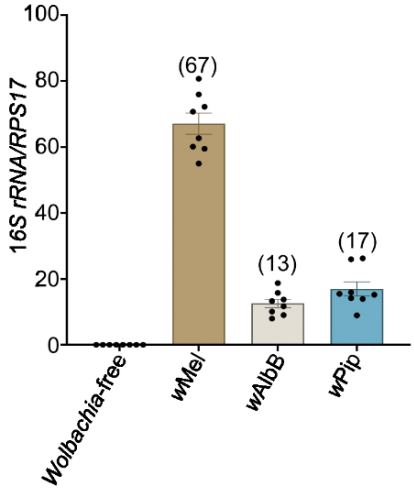

Supplementary Fig. 2: *Wolbachia* density in *Ae. aegypti* ovaries. Ovaries of at least 8 non-blood-fed female mosquitoes of Rockefeller (*Wolbachia*-free), Rockefeller-*w*Mel, Rockefeller-*w*AlbB, and Rockefeller-*w*Pip mosquito lines were dissected. *Wolbachia* per cell (in parentheses) was determined by qPCR (*Wolbachia 16S rRNA/RPS17*). Data are mean with ± Standard Error of the Mean (±SEM).

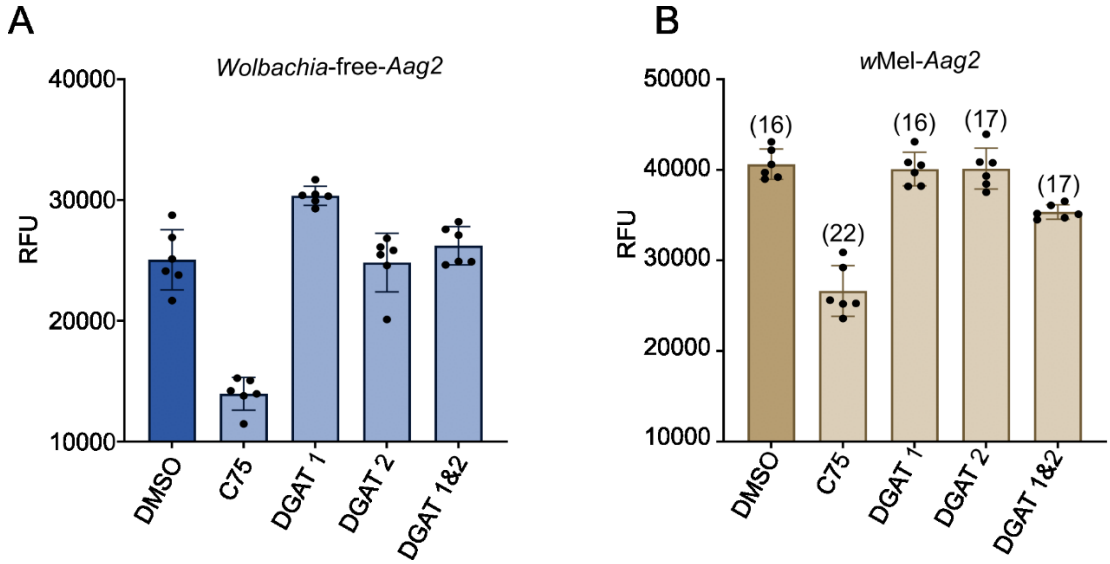

Supplementary Fig. 3: The Fatty Acid Synthase (FAS) inhibitor, C75, efficiently reduces LD accumulation in *Aag2* cell lines. (A) *Wolbachia*-free and (B) *w*Mel-*Aag2* cell lines were treated with C75, DGAT 1, DGAT 2, and DGAT 1&2 combined for 24 hours prior to LD staining. For live staining of LDs, cells were incubated with BODIPY 493/503 for 1 hour. The numbers in parentheses represent the average number of *Wolbachia* per cell (*Wolbachia 16S rRNA*/*RPS17*) after each treatment. Data are mean with ± Standard Deviation (SD) and represent 1 independent experiment with six biological replicates each. Fluorescence was detected with a microplate reader at 485/535 nm (excitation/emission) range. RFU – Relative fluorescence units.

SI References

1. McMeniman CJL, Roxanna V.; Cass, Bodil N.; Fong, Amy W.C.;, Sidhu MW, Yu-Feng; Scott L., O'Neill. . Stable Introduction of a Life-Shortening Wolbachia Infection into the Mosquito Aedes aegypti. *Science* **323**, (2009).

2. Kuno G. Early history of laboratory breeding of Aedes aegypti (Diptera: Culicidae) focusing on the origins and use of selected strains. *J Med Entomol* **47**, 957-971 (2010).